PROPPANT FRACTURE CONDUCTIVITY WITH HIGH PROPPANT LOADING AND HIGH CLOSURE STRESS

A Thesis

by

MATTHEW CHARLES RIVERS

Submitted to the Office of Graduate Studies of
Texas A&M University
in partial fulfillment of the requirements for the degree of

MASTER OF SCIENCE

May 2010

Major Subject: Petroleum Engineering

PROPPANT FRACTURE CONDUCTIVITY WITH HIGH PROPPANT LOADING AND HIGH CLOSURE STRESS

A Thesis

by

MATTHEW CHARLES RIVERS

Submitted to the Office of Graduate Studies of
Texas A&M University
in partial fulfillment of the requirements for the degree of

MASTER OF SCIENCE

Approved by:

Chair of Committee,	Ding Zhu
Committee Members,	A. Daniel Hill
	Yuefeng Sun
Head of Department,	Stephen A. Holditch

May 2010

Major Subject: Petroleum Engineering

ABSTRACT

Proppant Fracture Conductivity with High Proppant Loading and High Closure Stress.

(May 2010)

Matthew Charles Rivers, B.S., Michigan State University

Chair of Advisory Committee: Dr. Ding Zhu

Ultra-deepwater reservoirs are important unconventional reservoirs that hold the potential to produce billions of barrels of hydrocarbons, but also present major challenges. This type of reservoir is usually high pressure and high temperature (HPHT) and has a relatively high permeability. Hydraulic fracturing high permeability reservoirs are different from the hydraulic fracturing technology used in low permeability formations. The main purpose of hydraulic fracturing in low permeability reservoirs is to create a long, highly conductive path, whereas in high permeability formations hydraulic fracturing is used predominantly to bypass near wellbore formation damage, control sand production and reduce near wellbore pressure drop. Hydraulically fracturing these types of wells requires short fractures packed with high proppant concentrations. In addition, fracturing in high permeability reservoirs aims at achieving enough fracture length to increase productivity, especially when the viscosity of the reservoir fluid is high. In order to pump such a job and ensure long term productivity from the fracture, understanding the behavior of the fracture fluid and proppant is critical.

A series of laboratory experiments have been conducted to study conductivity and fracture width with high proppant loading, high temperature and high pressure. Proppant was manually placed in the fracture and fracture fluid was pumped through the pack. Conductivity was measured by pumping oil to simulate reservoir conditions. Proppant performance and fracture fluids, which carry the proppant into the fracture, and their subsequent clean-up during production, were studied. High strength proppant is ideal for deep fracture stimulations and in this study different proppant loadings at different stresses were tested to see the impact of crushing and fracture width reduction on fracture conductivity.

The preliminary test results indicated that oil at reservoir conditions improves clean-up of fracture fluid left in the proppant pack compared with using water at ambient temperature. Increasing the proppant concentration in the fracture showed higher conductivity values in some cases even at high closure stress. The increase in effective closure stress with high temperature resulted in a significant loss in conductivity. Additionally, the fracture width decreased with time and increased effective closure stress. Tests were also run to study the effect of cyclic loading which is expected to further decrease conductivity.

DEDICATION

This Thesis is dedicated to my parents, Chuck and Nancy, and my sister, Katie for all the love and support they have provided me throughout my life. I would also like to dedicate this work to my girlfriend, Molly, who always provided me with encouragement when difficulties were faced.

ACKNOWLEDGEMENTS

I would first like to acknowledge Dr. Ding Zhu and Dr. Dan Hill for giving me the opportunity to study under them and pursue my Master of Science degree. Their knowledge and encouragement has helped me understand the true value of education. When I first met Dr. Zhu I was considering pursuing a non-thesis masters degree, but she took the time to explain to me that I needed to do research and write a thesis. That advice provided me with an experience that I could not have imagined and for that I am very grateful.

Next, I would like to thank Dr. Yuefeng Sun for serving as my committee member. I would also like to thank John Maldonado, Maysam Pournik, Andres Pieve La Rosa, Juan Carlos Correa, Kevin Smith, and Heber Martinez for their help and support.

Also, I would like to thank the Harold Vance Department of Petroleum Engineering for giving me the opportunity to pursue my masters degree. The quality of the people who make this program work is, I believe, second to none.

Lastly, I would like to thank British Petroleum (BP) for funding this project. More specifically, I would like to thank the engineers at BP, Karen Olsen, A.V. Mahadev, Jennye Pusch, and Tom Luce, for their support during this project.

TABLE OF CONTENTS

CHAPTER Page

LIST OF FIGURES

FIGURE Page

LIST OF TABLES

CHAPTER I

INTRODUCTION

1.1 Hydraulic Fracturing in Ultra-deepwater Reservoirs

The decrease in conventional oil reserves combined with the increase in demand for hydrocarbons has led the industry to pursue the development of more unconventional reserves in order to fill the gap for demand. An unconventional reservoir contains oil and gas which usually requires a method of stimulation or drilling, i.e. hydraulically fractured or horizontally drilled to achieve a commercially economic production rate. Oil and gas produced from shale gas, tight gas sands, oil shale, and deepwater wells are all examples of unconventional reservoirs. These types of reservoirs are what have become, and will remain the driving force for increased technology.

Ultra-deepwater reservoirs have the potential to produce billions of barrels of hydrocarbons in deep buried formations. The reservoirs usually contain mainly oil and are very high in temperature and pressure. The attractive element is they are very high in permeability, sometimes in the Darcy range, providing very economic production rates. One major concern with higher permeability formations, however, is damage caused from drilling, or mud filtrate invasion which causes increased near wellbore pressure drop and consequent production loss. Another concern is sand production due to a lack of consolidation in the reservoir rock, and can possibly lead to the failure of very costly subsurface equipment. In lower permeability wells hydraulic fracturing is

---

This thesis follows the style of *SPE Production and Operations*.

used to create a high conductivity path deep into the formation in order to create an economical production rate. Hydraulic fracturing high permeability reservoirs, provides improved connectivity between the wellbore and reservoir by bypassing formation damage while pushing the formation back around the wellbore to act as a filter for sand control. An increase in productivity can also be achieved by hydraulically fracturing a longer fracture in high permeability reservoir.

The idea of hydraulic fracturing and gravel packing, known as frac-packing, for sand control was first put into practice in the 1970's in Venezuela. The fracture treatment was carried out using a viscous crude (10-20 cP) and sand sized to control formation sand. A screen was then washed down and sand was placed around it (Roodhart et al. 1994). A small number of frac-pack completions were performed in the early 1980's, and the number of completions increased in the late 1980's and early 1990's as the need increased and technology improved. The technique continued to gain popularity with successful implementations in various petroleum regions including the Gulf of Mexico, Prudhoe Bay (Alaska), Indonesia, Nigeria, Australia and the North Sea (Aggour 2001).

Operationally, fracturing high permeability formations are different from fracturing low permeability formations due to the expected high leak-off rate, which influences fracturing pressure as a function of time. In addition, because of the desired high fracture conductivity, the concept of tip screen-out is applied. In tip screen-out, the fracture is designed in such a way that by the time the fracture reaches the desired length the loading pad volume has leaked off into the formation. After the pad volume has

leaked off, the presence of the proppant laden fluid at the leading edge of the fracture initiates the screen out process. Continued injection of the proppant laden fluid causes the fracture to widen and balloon, reaching a greater than average width and high proppant concentration. The fracturing pressure then sharply increases causing the proppant to pack around the wellbore. (Hunt et al. 1994)

In order to ensure a successful hydraulic fracture, the fracturing fluid must exhibit several desirable properties. The fluid must cause minimum damage to the formation, have good proppant carrying capacity, minimally affect the conductivity of the proppant pack, and minimize fluid loss. Currently, many different types of fracturing fluids are used with the most common being salt-based polymers with the use of cross-linkers.

It was not until the early 1970's that cross-linkers were introduced with the purpose of increasing the viscosity of gelled water base fracturing fluids. The increased viscosity could be achieved without increasing the polymer concentration helping carry proppant downhole into the fracture. In addition, different kinds of additives have also been used in fracturing fluids to compensate for different reservoir conditions such as high temperature, presence of clay, extensive pumping time, etc.

Considering the high costs involved in drilling, completing and producing ultra deepwater wells, it is important to optimize the hydraulic fracture job of each well to ensure economic production. Understanding some of the issues leading to the loss of productivity and implementing ways to counteract them becomes a very important issue.

1.2 Literature Review

Many in the industry mistakenly use reference conductivities and/or crush measurements as their guide for proppant selection and fracture design. Yet the industry continues to struggle with well testing and production data analysis results that indicate disappointing effective static half-lengths and short flowing apparent fracture half-lengths, when in fact it is known that the fracture treatments created much longer fracture measurements. One approach to estimating fracture conductivity realistically is by conductivity testing in a laboratory providing as many realistic damage factors as possible. (Palisch et al. 2007)

The early standard procedure for measuring short-term conductivity of proppant packs was developed by the American Petroleum Institute (API) using a Cooke Conductivity Cell. This was documented in API-61 (1989). For years, this procedure along with a few revisions came to become the standard for long-term testing of proppant packs. In 1987, Stimlab made three changes on API RP 61 to get better results (Much and Penny 1987). Instead of the steel pistons, Ohio sandstones were used; the temperature was changed to either 150°F or 250°F and a known proppant concentration (generally 2 lb/ft^2) was placed between the cores with stress maintained for 50 hours. It was found that these changes reduced the measured conductivity by as much as 85% depending on proppant quality and test conditions (Palisch et al. 2007). In 2007, this standard for long-term testing came to be known as the ISO 13503-5 (Kaufman et al. 2007).

McDaniel (1986) conducted a series of experiments evaluating the effect of subjecting proppant to extended periods at different closures stresses and varying temperature between 75 °F and 275 °F. Laboratory tests of conductivity at ambient temperature and short times were found to be optimistic and when severe test conditions were held for 10 to 14 days, a correction factor of 0.47 to 0.54 had to be used for synthetic proppants.

Freeman et al. (2009) studied the effect of high temperature, closure stress and fluid saturation on proppant crushing. Two crush resistance tests were performed using high strength bauxite at 15,000 and 20,000 psi and 400 ºF and 500 ºF. It was found that pressurized fluid saturation, increased temperature and extended stress loading, increase the occurrence of proppant failure.

Stephens et al. (2007) performed a series of experiments to study the behavior of proppants under cyclic stress to simulate a typical environment where there are multiple shut-in and drawdown cycles. Crush resistance tests at 6,000, 8,000, and 10,000 psi were performed using bauxite and kaolin clay proppant. It was shown that the stress cycles significantly changed the size distribution with each cycle; however, the greatest change generally occurred during the first five cycles.

At present, there is significant information available on the behavior of low proppant concentration packs at temperatures and pressures equivalent to ultra deepwater reservoirs. However, there is very little data on the behavior of high proppant concentration packs at different closure stress. In addition, the use of 2% KCl to simulate reservoir fluid and gel clean-up is not very accurate. This research, therefore,

will conduct a series of experiments using a 10 cp mineral oil to study gel clean-up in the proppant pack, the behavior of high proppant concentrations at different closure stresses and identify the effect of crushing and embedment on long term conductivity in these packs. Tests will also be run to study the cyclic loading of the proppant as a behavior of well shut-in and drawdown.

1.3 Problem Description

With the extremely high costs associated with developing ultra deepwater reservoirs, maintaining economic long term production becomes a key component in deciding to go forward with a project. Fracture conductivity and fracture width are two of the more important attributes that determine the success of a fracturing treatment in high permeability formations.

Fracture conductivity is affected by many variables such as gel polymer type, proppant type, proppant concentration, and effective closure stress. Different polymers are chosen for stimulation because of their ability to increase and hold fluid viscosity at different temperatures and pressures, thereby helping in proppant transport from the surface to the fracture tip. However, it is also known that the cross-linked polymer chains are difficult to breakdown which can damage/reduce the formation's permeability and proppant pack conductivity. In deep reservoirs, the mechanical properties of the proppants are tested at higher closure stresses which sometimes lead to proppant crushing and embedment, lowering long term conductivity. The lower conductivity equates to lower productivity in a high permeability formation.

There are publications that study long term conductivity of fractures at different closure stresses, but there are a lack of publications which test these proppants under realistic stimulation conditions, with cross-linked fracture fluid, at high temperature and with mineral oil for clean up. Additionally, there is a lack of data comparing fracture performance of resin coated proppant to equivalent uncoated proppant. Coated proppant was initially developed to reduce proppant flowback during production, which creates a fracture width reduction due to a loss of proppant at the entrance of the fracture resulting in near wellbore pressure drop. The width reduction can act as a choke limiting production from the entire fracture (Barmatov et al. 2008). Proppant that flows back can also have a detrimental effect on production equipment and lead to plugging or erosion of downhole completions.

In this study, laboratory tests will be carried out using different concentrations and types of high-strength proppant to study the effects of increasing proppant pack closure stress and its effect on fracture conductivity. An experimental apparatus will be developed to simulate fracturing conditions of ultra deepwater wells and the fracture fluids and proppant will be examined for their effect on fracture conductivity. Gel damage in the fracture/proppant pack will be investigated and long term fracture conductivity will be measured to identify the treatment conditions resulting in sustained fracture conductivity. The test will measure the clean-up efficiency of the gel, long-term conductivity of the proppant pack, and the effects of cyclic stress on fracture conductivity.

1.4 Research Objective

This research had three main objectives:

1. Set up an experimental apparatus and procedure that will be used to study the behavior of fracture conductivity under simulated reservoir conditions. High temperature mineral oil is pumped through the cell to simulate reservoir flow and measure conductivity.
2. Conduct experiments to see the effect of closure stress and high proppant concentrations on conductivity.
3. Observe fracture width simultaneous to measuring long term conductivity at increasing or cyclic closure stresses.
4. Compare coated and uncoated proppant fracture conductivity under cyclic and long term loading conditions.

By achieving the above objectives, this research was able to predict with higher accuracy the long term conductivity of a high permeability hydraulic fracture completion for a well drilled in an ultra deepwater reservoir. Additionally, this study aids in the further testing of proppant packs of varying proppant concentrations and types (coated and uncoated) with conditions such as higher temperatures, closure and cyclic stresses, and fracture fluids that accurately represent reservoir conditions and the planned stimulation job.

CHAPTER II

EXPERIMENTAL SET UP, PROCEDURES, AND CONDITIONS

2.1 Experimental Apparatus

In 1989, API adopted a standardized conductivity measurement apparatus, called a conductivity cell, to provide comparable and repeatable results from tests conducted by different labs. In this procedure proppant was placed manually between the core samples and conductivity measurements were taken by pumping a fluid through the conductivity cell measuring differential pressure across the cell. To further accurately represent field conditions, fracture fluid was pumped through the proppant pack with cross-linker and breakers. The purpose of developing such a setup was to provide appropriate scaling to symbolize field conditions experimentally with flexibility for further studies of gel damage, fluid cleanup and proppant behavior.

The conductivity apparatus for this study was used to simulate the following four conditions:

- Fracture fluid pumping
- Simulated oil production
- Fracture width
- Fracture conductivity

2.1.1 Fracture Fluid Pumping

The fracture fluid pumping apparatus consists of the following: (**Fig. 2.1**)

- 5 gallon bucket and paddle mixer - to prepare the cross-linked fluid
- Randolph Austin peristaltic pump
- Heating jacket - to increase the cell temperature to reservoir conditions
- Modified API RP-61 fracture conductivity cell (API 1989)
- Load frame to apply a designed load stress
- Fraction leak off fluid collector
- Pressure Transducers
- Data acquisition system
- Waste bucket

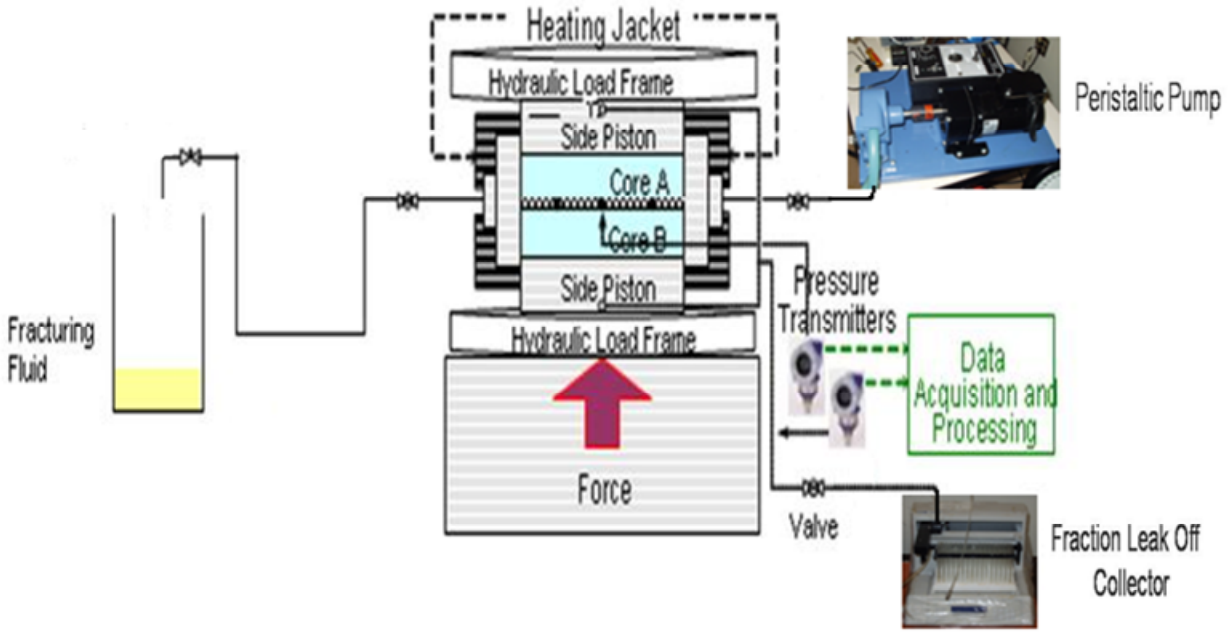

Fig. 2.1—Pumping schematic of fracture fluid pumping

Fig. 2.1 shows a schematic of the fracture fluid pumping system used for the experiment. The fluid was mixed in a 5 gallon bucket using a simple paddle mixer. Once the fluid was hydrated and all the buffers, breakers, and cross linker were added and mixed, the bucket was moved over to the peristaltic pump and pumping through the cell/ proppant pack began. During pumping, the cell was heated using a heating jacket and the fracture fluid was collected in a separate bucket at the outlet of the cell. Leak off was also collected and in certain cases measured using a fraction collector to determine leak off coefficients. Pressure could also be monitored and kept constant to ensure an accurate leak off measurement.

2.1.2 Simulated Oil Production

The apparatus that is used to simulate oil production and measure fracture conductivity through the cell contains:

- Oil bath – Labnics 1000T
- Micro Pump variable speed positive displacement gear pump
- Kobold DOM positive displacement flow meter with digital MRT-1533 display
- Thermocouple
- Acuity AR200-25 laser displacement sensor
- A modified API RP-61 fracture conductivity cell
- Load frame
- Pressure transducers
- Data acquisition system

The schematic of the apparatus for conductivity measurements is shown in **Fig. 2.2**. Mineral oil is used in the experiment as the reservoir fluid and heated by an oil bath to achieve the desired viscosity and flowing temperature. The mineral oil was circulated through the cell in a loop via a variable speed positive displacement pump back to the oil bath. Flowing temperature of the oil is measured using a thermocouple placed at the inlet of the cell and a heating jacket is used to heat the cell to reservoir condition temperature. Fracture conductivity is calculated by flowing oil through the proppant pack between the core samples and measuring pressure differential under different stress conditions created by the load frame. The pressure differential measurements are taken by pressure transducers and recorded by a data acquisition system for up to 24 hours to see the long-term decline in conductivity at certain stress conditions. Parallel with the pressure data, flow rate is also measured using a flow meter and recorded.

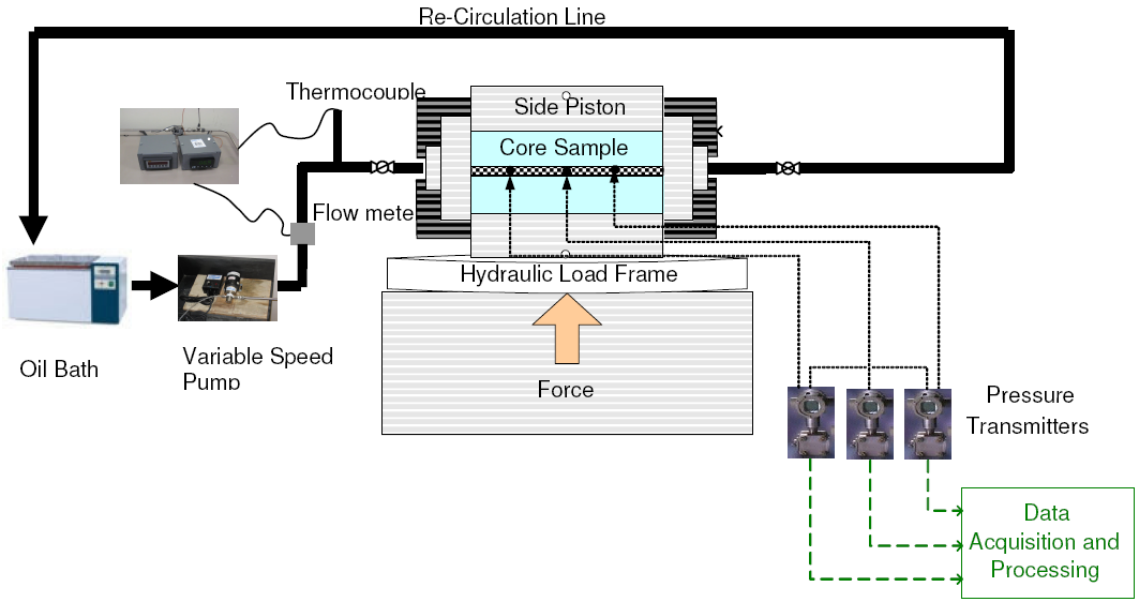

Fig. 2.2—Schematic of fracture conductivity apparatus

Fig. 2.3 shows the modified API RP-61 conductivity test cell and a typical core sample. Dimensions of the cell body are 10 in. long, 3-1/4 in. wide and 8 in. tall. The top and bottom pistons in the cell (3 in. tall), with viton polypack seals, are used to keep the cores in place, hold leak off pressure and prevent any leakage. Leak off fluid during pumping travels through the cores to channels milled into the contacting surface of the pistons shown in **Fig. 2.4**. The pistons have a pilot hole drilled through the center that connects to the leak off flow lines. The cell is made of 316 grade stainless steel and has been milled to accommodate the exact dimensions of the silicone surrounded core samples. The dimensions of a core samples with the silicone surround are 7-1/4 in. long, 1-3/4 in. wide and 3 in. tall.

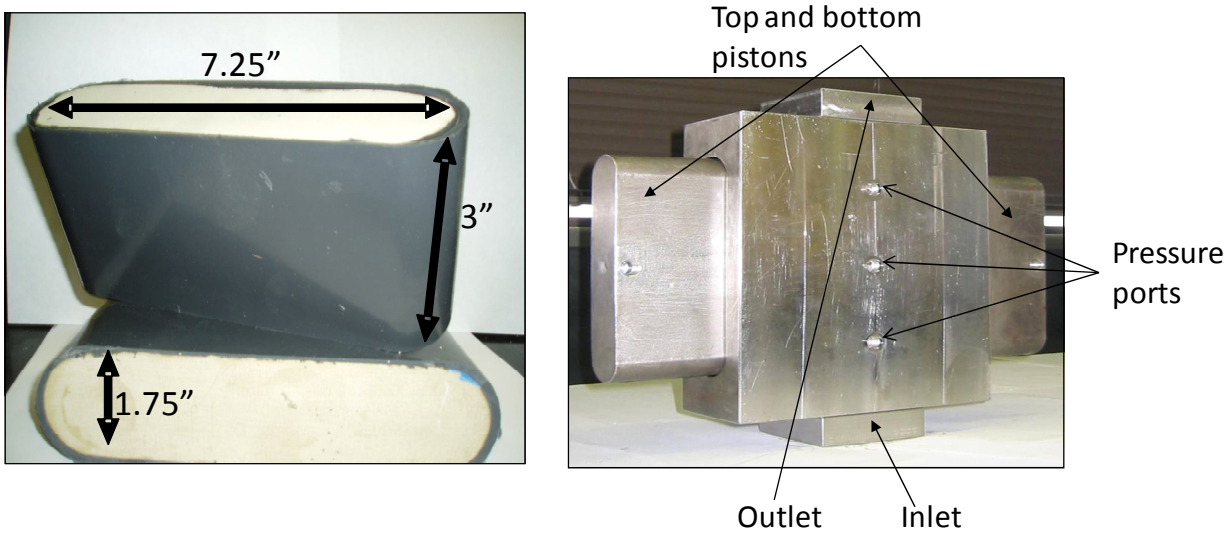

Fig. 2.3—Conductivity cell and core samples used for experiment

Flow inserts with o-rings around the perimeters and screens inside of them are used to keep the proppant in place during the experiment. The inserts have male-male NPT fittings fastened to them to connect the flow lines for the inlet and outlet of the cell. To measure conductivity, the pressure difference across the cell is measured using the outer two pressure ports, while the middle port measures absolute or cell pressure. The pressure ports have fittings mounted to them which attach to the lines of the pressure transducers. A hydraulic load frame is used to provide the closure stress on the pistons for each test.

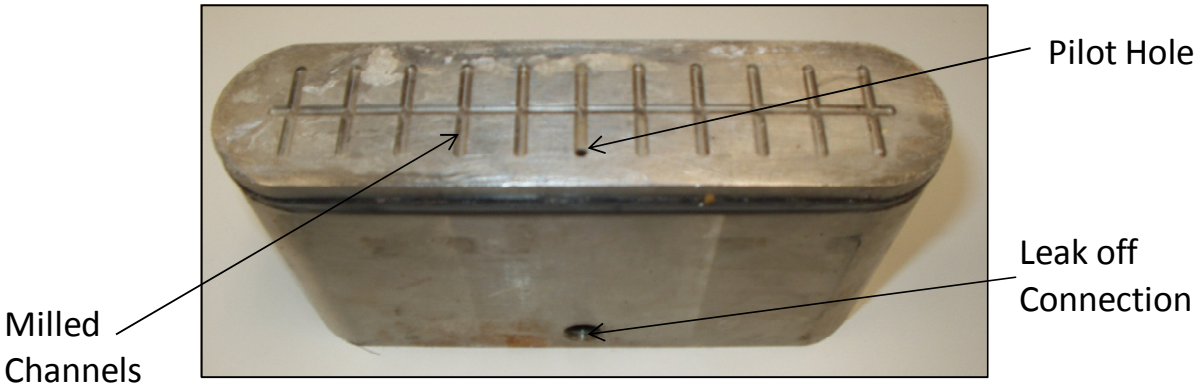

Fig. 2.4—Piston (top or bottom) for conductivity cell

2.1.3 Fracture Width

The experimental setup also is capable of measuring the fracture width dynamically during pressure differential measurement. The displacement of the load frame piston is measured using an Acuity AR200-25 laser displacement sensor (**Fig. 2.5**) and wired to the data acquisition system parallel with the flow meter and pressure transducers. The laser can be rotated and moved vertically for calibration enabling the ability to compare width and conductivity of the fracture.

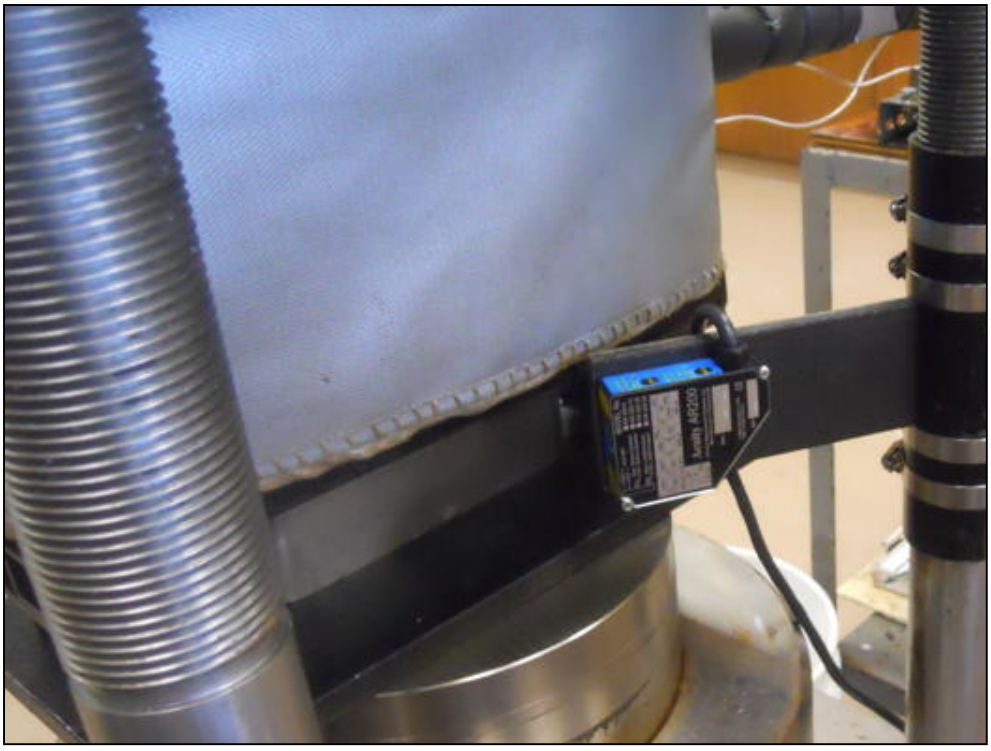

Fig. 2.5—Fracture width displacement laser

2.1.4 Surface Characterization

The profilometer apparatus (**Fig. 2.6**) is used to characterize the surface profile of the rock. A profilometer is a precision vertical distance measurement device which can measure small surface variations in vertical surface topography as a function of the surface position. The vertical measurement is made with a laser displacement sensor while the sample is moved along its length with the help of a moving table. This measurement is repeated several times over the length of the sample to cover the entire surface area.

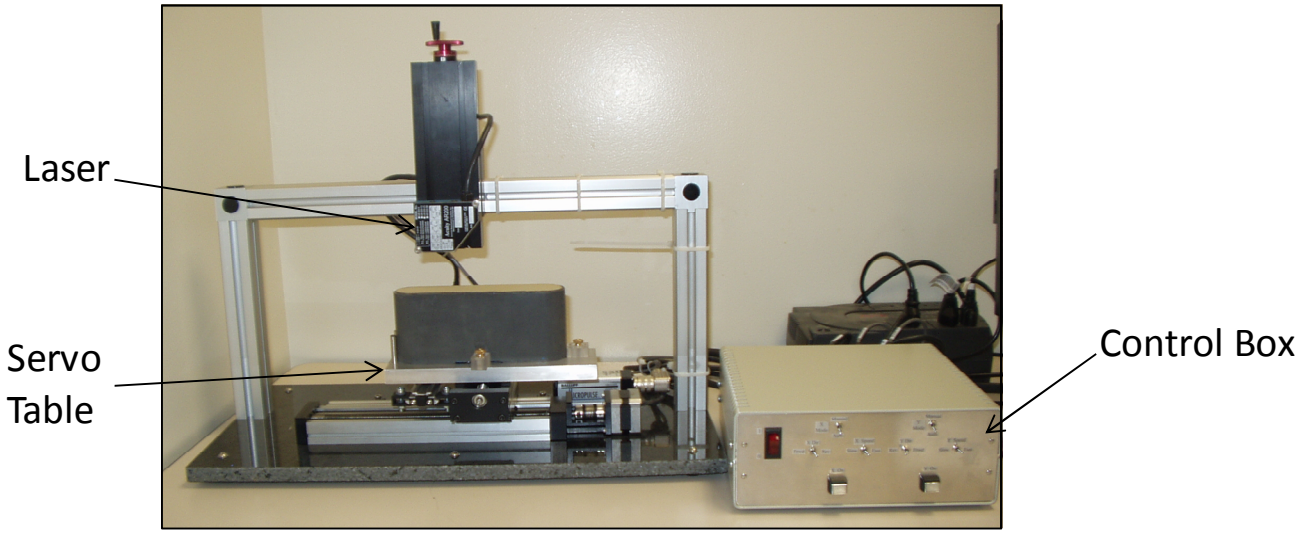

Fig. 2.6—Profilometer device

In this experiment, the surface scanning of the cores was performed before and after conductivity measurements. The surface profile difference was studied to observe the extent of proppant embedment and core erosion.

2.2 Experimental Procedure

The experimental procedure consists of six main steps as shown in **Fig. 2.7** listed below.

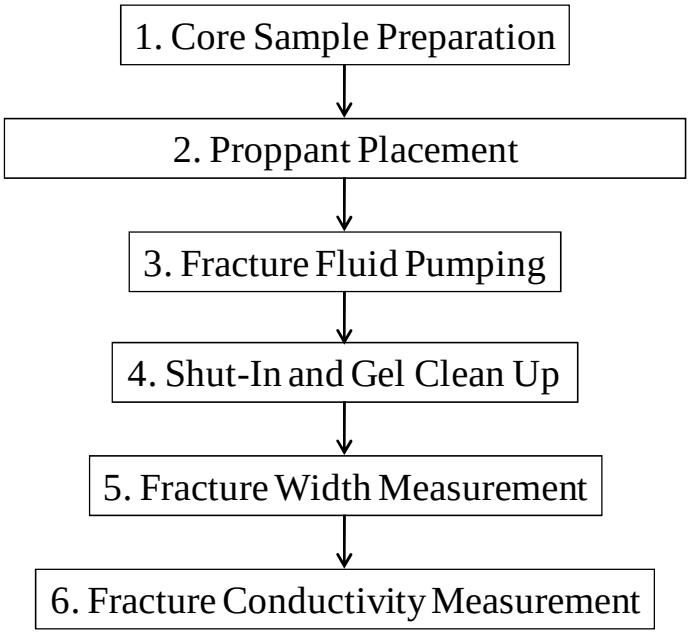

Fig. 2.7—Experimental steps for fracture conductivity measurement

2.2.1 Core Sample Preparation (Berea Sandstone)

The core sample used initially in this experiment was Berea sandstone. This rock was chosen because of its high permeability and strength, which closely represents the reservoir in this study. The rock samples were custom cut into a rectangular shape with round edges using a masonry table saw with a diamond impregnated blade. To provide a perfect fit and better seal inside the conductivity cell the core samples were surrounded

with a silicone-base sealant. Core samples before and after with silicone rubber are shown in **Fig. 2.8**.

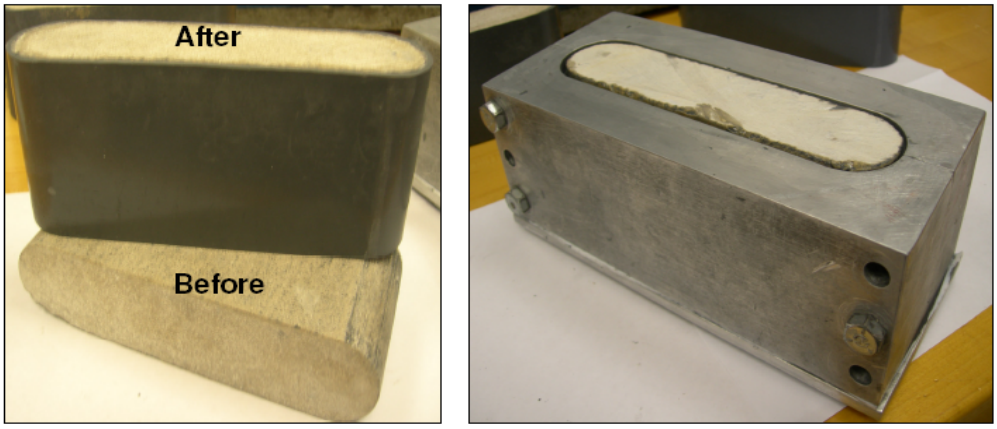

Fig. 2.8—Core samples and mold used for core sample preparation

The procedure to prepare the core samples is as follows:

1. Prepare and clean the rock samples that need to be molded.
2. Put 3M blue painters tape on the top and bottom of the core sample, cutting the edges with a razor cutter.
3. Apply silicone primer (SS415501P), about three times with a brush, along the edges of the core samples. Allow 15 minutes waiting time in between primer applications.
4. The mold, shown in Fig. 2.8, is made of stainless steel, with a plastic bottom. Clean the metal surface and bottom plastic piece of the mold with acetone using a cloth.

5. Spray silicon mold release S00315 on the metal molds three (3) times. Wait for two (2) minutes between each spray.
6. Assemble the mold. Tighten the four bolts at the bottom and the three bolts on the side. Make sure all bolts are tight.
7. Put the rock in the mold and adjust to center position.
8. Prepare 75 cc of silicone potting compound and 75cc of silicon curing agent from the RTV 627 022 kit for a 1:1 mixing ratio. Weigh before mixing both components to ensure that the mixture is 50/50 of each component, either by volume or by weight percent. Mix and stir thoroughly.
9. With a disposal beaker pour the mixture in the gap between the core and the mold carefully until the silicone fills to the top of the core sample.
10. Let mold set for 24 hours in an area of at least room temperature.
11. Unscrew all the bolts from the mold and carefully remove the samples from the mold using a c-clamp.
12. Cut extra silicon on the edges with a razor cutter.
13. Remove blue painters tape from core surfaces.
14. Label the rock sample. The core sample is ready to use.
15. The core samples initially are saturated with air. Two to three hours prior to running an experiment, the core samples are saturated with the base fluid (12.3 ppg NaBr) using the vacuum pump and bowl as shown in **Fig. 2.9**. The procedure to do this is as follows:
    a. Clean the beaker to remove any old fluid and solids.

b. Fill the beaker with 2.5 L of base fluid (in this case 12.3 ppg NaBr)

c. Place the clean core samples in the beaker. *The core samples must be fully submerged.*

d. Apply vacuum grease along the rim of the beaker and press the lid down. *Make sure the lid is sealed.*

e. Turn on the pump. *Check to see if bubbles are coming out of the core sample. Run this pump for only 2-3 hours.*

Fig. 2.9—Core saturation vacuum pump

2.2.2 Fracture Width Calibration

In order to measure the fracture width accurately the laser displacement sensor had to be adjusted a certain range of distance from the load frame piston. A square tube was cut to 14 ½ inches in length and placed in the load frame to replicate the point at which the fracture width was zero as shown in **Fig. 2.10**. Each piston has a height of 4 inches and each core has a height of 3 inches giving the cell assembly a height of 14 inches. In addition, the stand for the cell has a plate thickness of a half an inch giving the total assembly a height of 14 ½ inches with no proppant pack in between the cores. This matches the square tube height.

The laser has an optimum span of 1 inch and a sweet spot distance of 1.339 inches giving an optimum range of between 0.839 and 1.839 inches. Therefore, when calibrating the laser a distance of approximately 0.900 inches was selected to represent zero fracture width offering the capability to measure almost a 1 inch wide fracture. Once actual measurement began with the cell in the load frame the measurement taken by the laser could be subtracted by the calibrated measurement to get the actual fracture width.

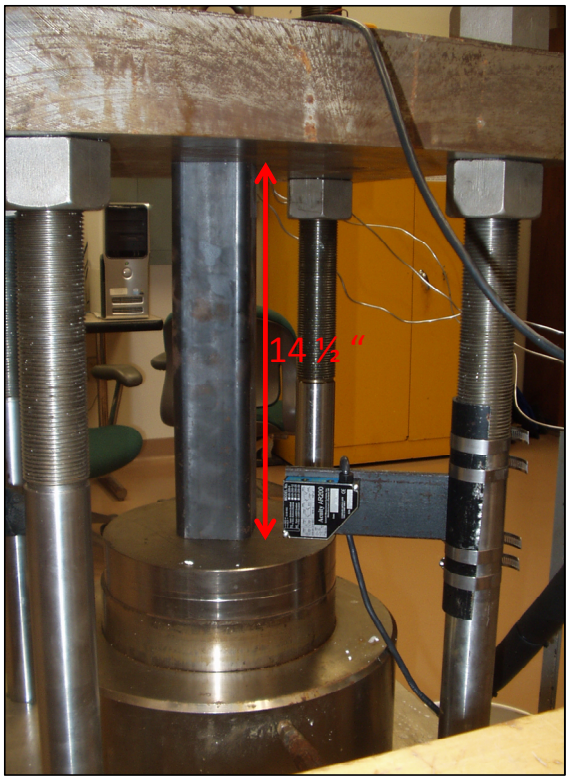

Fig. 2.10—Fracture calibration beam

2.2.3 Proppant Placement

In these experiments, proppant placement between the core samples was done manually. The detailed procedure for setting up the conductivity cell prior to pumping is as follows:

1. Prepare the core samples. Follow the guideline in section 2.2.1. *Only use the side of the core that has the silicon epoxy coating flush with the core sample as the fracture face. Any grooves can lead to errors in conductivity readings.*

2. Wrap each core with two rows of Teflon tape, one near the top and the other near the bottom, and apply vacuum grease around each row. This helps provide a seal once inside the cell.
3. Insert the bottom core sample into the bottom opening of the conductivity cell using the hydraulic jack. This core will serve as the lower fracture face in the cell. Make sure the lower fracture face lines up with the bottom of the pressure ports in the cell. This ensures that the proppant pack is in the center of the cell and both cores and side pistons can fit in properly with a good seal.
4. Put the conductivity cell on the stand with the bottom piston upright inside the stand. Make sure the leak off valve is open to prevent air from being trapped between the piston and core. Check to see that the seal on the bottom piston is inside the cell. *Note: all rubber seals must be coated with a film of high temperature o-ring grease to ensure a good seal.*
5. Adjust the bolts on the stand to fit the bottom piston so that the cell body is flush and the piston is contacting the bottom core.
6. Place the screen (30 mesh) in flow insert #2 (outlet side of the cell) to prevent loss of proppant.
7. Put the side flow inserts into the cell with the numbers on the inserts matching the numbers on the cell.
8. Measure the desired amount of proppant and place evenly on the lower fracture face.
9. Put the conductivity cell with the stand in the center of the hydraulic load frame.

10. Activate the AP-1000 hydraulic pump by opening the air supply valve. Open the air regulator and adjust the supply pressure to move the bottom ram of the hydraulic load frame up or down.
11. Insert the top core sample into the conductivity cell using the hydraulic frame.
12. Place the top piston into the cell. Apply approximately 500 psi on the cell to keep the pistons inside the cell.
13. Connect all pumping, leak off and pressure lines onto the conductivity cell. *Make sure all connections are tight.*
14. The setup should now resemble **Fig 2.11.**

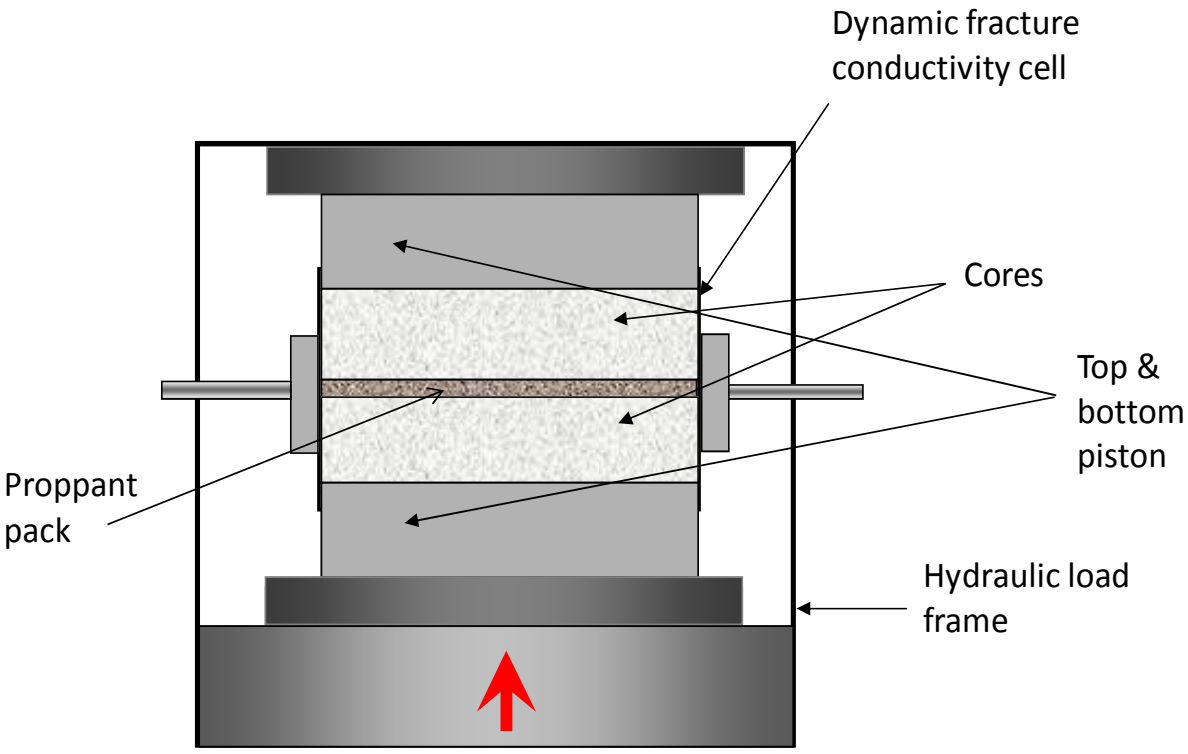

Fig. 2.11—Diagram of assembled cell in load frame

15. Wrap the heating jacket around the conductivity cell.
16. Set the temperature controller of the heating jacket to a predetermined temperature (350°F). Turn on the controller to heat up the heater. *Note: due to a large amount of heat loss through conduction between the heating jacket and cell the cell must be preheated at a higher temperature for several hours.*
17. The setup is now ready for pumping.

2.2.4 Fracture Fluid Mixing and Pumping

A service company designing the fracture fluid for this project provided the chemicals that are used in this experiment. During the experiment, the fracture fluid is mixed simultaneous to setting up the cell. Below is the general mixing procedure for the fracture fluid:

1. Add 2 gallons of tap water into the mixing bucket.
2. Add 3,593 grams of Sodium Bromide (NaBr) to bucket to make 12.3 ppg NaBr brine. Add 0.8 cc of BF-10L buffer and mix for 60 seconds. Once the buffer is added the pH of the mixture should be about 6.5.
3. Mix the brine solution until NaBr has completely dissolved and then add 83 cc of concentrated polymer guar (GW-3LE) into the mixing bucket. Mix base gel for 30 minutes to allow the gel adequate hydration time.
4. Slowly add 11 cc of pH Buffer (BF-11L) to the hydrated fluid.
5. Add in 76 cc of the mixture of XLW-56/C12 to bucket. This delays the cross linking. *Before starting the experiment, setup the XLW-56/C12 mixture using*

NaOH and XLW-56 in the ratio of l NaOH : 8.33 XLW-56. The reaction is exothermic and hence should be mixed slowly not allowing the temperature to exceed 110F.

6. Finally, 61 cc of breaker (GBW-24L) and 91 cc of buffer (BF-9L) are mixed into the bucket. Mix for about 1 – 2 minutes before pumping.

Once the fluid has been mixed it is important to begin pumping immediately so the fluid does not cross link before it has all been pumped through the cell. If the fluid crosslink's prematurely, the pump will not be able to supply enough pressure to pump the fluid through the proppant pack. The fraction collector must also be set up prior to pumping and in this experiment is set at a 0.5 min/tube collection rate. The pumping and leak off procedure is as follows:

1. Make sure all test tubes in the fraction collector are clean and dry.
2. Place the inlet hose of the peristaltic pump in the bucket of mixed fracture fluid and begin pumping. Make sure all valves are open to allow flow through cell and into waste bucket.
3. Start the fraction collector to begin measuring leak off. Make sure the valve on the leak off line is in the open position
4. Adjust the pump speed to maintain a cell pressure of 25 psi.
5. Once all or most of the fracture fluid has been pumped, turn pump and fraction collector off.
6. Close the leak off valve.

7. Measure the leak off in each tube of the fraction collector either by volume or by weight.
8. Continue heating the cell with the heating jacket set at 350°F. It will take an hour for the cell to reach 235°F.

To calculate the leak off coefficient (C) from the data collected, a plot of cumulative volume vs. the square root of time must be generated with units of cubit feet and minutes respectively. Once the chart has been created, the slope (m) of the later points where the trend of the data becomes linear after the spurt data is used in Eq. 2.1.

$$m = \frac{1}{2} * C * A \tag{2.1}$$

The surface area (A) is the top and bottom surfaces of the cores or fracture face which is 0.17 ft^2.

2.2.5 Shut-In and Subsequent Gel Clean-Up

The fracture fluid is set up to break after two and half hours once heated to 235°F. A shut-in time of 4 hours is used for this experiment to allow time for the cell to heat up and sustain the 235°F for at least two and half hours. Periodically the cell temperature can be checked using an infrared temperature probe to ensure the proper heating jacket temperature. During the shut-in process, the heating jacket is set at 350°F for the entire 4 hours. It is also important to turn the oil bath on and set it to 132°C (270°F) to ensure that the mineral oil is heated up to temperature before the gel clean-up process.

Once the cell has been shut-in and heated for 4 hours and the mineral oil has reached temperature the gel clean-up process begins. The gel clean-up procedure is as follows:

1. Increase the closure stress to 3,000 psi at a rate of 150 psi/min.
2. Close the valve for the peristaltic pump and open the valve for oil flow.
3. Switch the valves downstream of the cell to allow the oil to flow into the waste bucket and not re-circulate into the oil bath (this will be the same as when the fracture fluid was pumped).
4. Open the bypass valve that will enable the fracture fluid in the line upstream of the cell to be pumped out into a waste bucket by the hot oil.
5. Turn on the positive displacement oil pump on and begin increasing the speed until the flow meter begins registering a flow rate.
6. Increase the pump speed until flow rate reaches 0.2 l/m.
7. Close the bypass valve after 1-2 minutes of flowing oil.
8. Continue flowing at 0.2 l/m until clean oil is flowing into waste bucket downstream of the cell.
9. Switch the downstream valves to begin re-circulation of the oil into oil bath.
10. Continue flowing until the temperature has reached 210°F. *Note: as the tubing begins to heat up, the temperature of the oil bath will need to be gradually lowered to maintain an equilibrium flowing temperature.*

2.2.6 Fracture Conductivity Measurement

Mineral oil with a viscosity of 10 cp is used to simulate oil production and measure fracture conductivity. The conductivity is measured for long periods of time at different closure stresses to study decline over time. The procedures to measure conductivity are as follows:

1. Bleed the pressure transducer lines where they hook up to the pressure transducers by cracking the lines. This will ensure that there is no air in the lines and minimize error in the pressure readings. *There are four transducers attached to the setup. Transducer A measures cell pressure, Transducers B (0-30 psi), D (0-10 psi) and C (0-1500 psi) measure pressure differential. Depending on the expected pressure differential use the smallest range to avoid error. Transducer B has a range of 0-30 psi and is the preferred transducer for measuring pressure differential for this experiment.*
2. Adjust the pressure on AP-1000 hydraulic pump to maintain a 3,000 psi closure stress acting on the fracture. Conductivity measurements are taken at 3,000 psi, 5,000 psi, 8,000 psi and 10,000 psi. *Attention should be paid to the closure stress as it tends to increase as the cell heats up during conductivity measurement.*
3. Open LabView to begin recording the pressure differential across the cell, flow rate, and fracture width. Open file “HydConductivityPressuresFlowWidth.vi” from folder “C:/LabView Programs/Hydraulic Fracturing/” and start recording data. LabView has already been calibrated for transducers B (0-30 psi), A (0-125

psi), flow rate (L/m), and fracture width (in.). The fracture width displayed in Labview will be the measured distance from the load frame piston and will need to have the calibrated value subtracted from it as described in section 2.2.3. Open Excel file "HydConductivityPressures.xls" from the same folder. In the Excel Sheet, Column D displays values for transducer B and Column C displays pressures for transducer D. *Record pressure from the start of pumping.*

4. Record pressure data at each stress level until the change is small (Approximately 20 hours).
5. After running all tests disconnect all lines to the conductivity cell.
6. Lower the load frame pressure to allow the removal of the conductivity cell.
7. Remove the rock sample from the cell with the cell stand and hydraulic frame.

To calculate the fracture conductivity from the experimental data, Darcy's law (Eq. 2.2) was used with the measured flow rate and pressure change.

$$k_f w = \frac{\mu * q * L}{h * \Delta p} * 8035.97 \tag{2.2}$$

The pressure drop (Δp) and flow rate (q) were recorded by LabView every 10 seconds at each closure stress. **Table 2.1** shows the values of the remaining constants used in the fracture conductivity calculation.

Table 2.1—Experimental constants used to conductivity equation

Conductivity Constants		
μ	Oil Viscosity, cP	10
L	Length of Fracture, in.	5.25
h	Height of Fracture, in.	1.75

2.3 Experimental Conditions

In this experimental study, Berea sandstone was used to study the effect of increasing closure stress on fracture conductivity. In order to simulate field conditions as accurately as possible and obtain valuable test results certain test parameters were taken into account. The following test conditions were adopted for this experiment.

- Fracture Fluid
- Proppant Type and Concentration
- Mineral Oil
- Temperature
- Cyclic Stress Conditions

2.3.1 Fracture Fluid Composition and Conditioning

A fracturing fluid composition is provided by a service company for this experiment. The fracturing fluid is selected by the operator to simulate realistic leak off, filter cake and gel damage conditions inside the conductivity cell and proppant pack. 12.3 ppg NaBr brine is the base fluid and guar polymer is used as a base gel for this experiment. All experiments are conducted at room temperature during the fluid preparation. The composition of the fracturing fluids used for the series of experiments is shown in **Table 2.2** below.

Table 2.2—Main components of fracturing fluid

Chemical	Condition
Hydration Buffer, pH	6.5
Guar Polymer, lb/Mgal	43.6
Buffer, pH	9.5-10.2
Breaker, GPT	8
Borate Crosslinker, GPT	10

* GPT = gal/Mgal of fluid

The components for the selected fracturing fluid are as follows:

1. Guar. Concentrated polymer guar is used to form a viscous base gel fluid.
2. pH Buffer. Is used to control pH which is important for polymer hydration rate and crosslinking rate.
3. Breaker. The purpose of breaker is to reduce the viscosity of the polymer solution after it has crosslinked and provide rapid fluid clean up.
4. Crosslinker. To increase gel viscosity and simulate field conditions.

2.3.2 Proppant Size and Concentration

Proppant used in this experiment is high strength proppant with a mesh size of 16/30. Two different types of ceramic proppant were used, uncoated and resin coated. High strength proppant is either ceramic or sintered bauxite, both of which are capable of handling stresses exceeding 10,000 psi. As this experiment studied fracture conductivity of proppant packs at different closure stresses, the proppant concentration was varied with each experiment. Proppant concentrations were varied between 4 lb/ft^2 and 8 lb/ft^2 to achieve the objectives of this research.

2.3.3 Mineral Oil Selection

To perform conductivity analysis of different proppant packs in these experiments, mineral oil with a viscosity of 10 cP at reservoir temperature was chosen. Mobile DTE Extra Heavy was the mineral oil selected. This was done to closely represent the reservoir fluid in the formation being studied. **Fig. 2.12** below displays the viscosity curve for the oil.

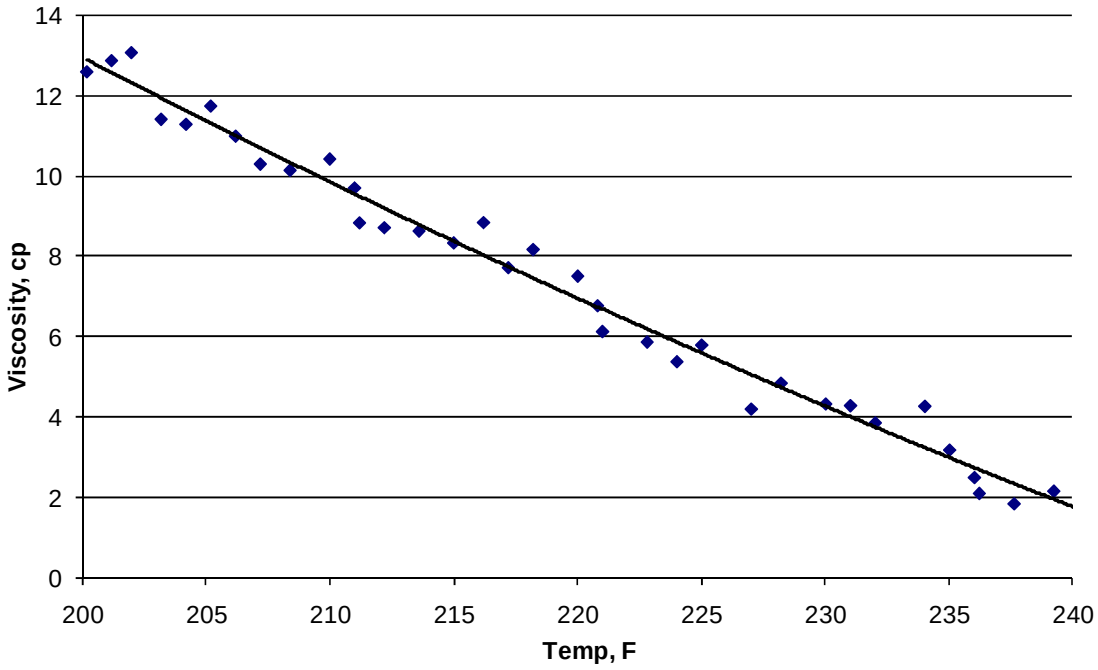

Fig. 2.12—Viscosity curve for mineral oil (200°F - 240°F)

2.3.4 Temperature

Temperature affects the breaking time of the gel and also the mechanical properties of the proppant. For this series of experiments, 235°F has been selected as the cell temperature and 210°F as the temperature of the oil. This is done to replicate the reservoir conditions of the oil and the conditions in the cell.

2.3.5 Mineral Oil Flow Rate

Mineral oil was used in these experiments to simulate oil production from the fracture into the wellbore. A flow rate for the laboratory setup was calculated to simulate a field production rate of 7000 Bbl/D using the values from **Table 2.3** below.

Table 2.3—Comparison of laboratory and field conditions

	Laboratory	Field
Fracture Height, ft	0.142	300
Fracture Width, in	0.7	0.8
Temperature, °F	235	235

To convert the field rate into the lab flow rate the values from Table 2.3 are used. The flow rate in one wing of the fracture is first calculated for a total production rate of 7000 bbl/d.

$$q_{1-wing} = \frac{7{,}000\frac{bbl}{d} * 158.987\frac{l}{bbl}}{24*60\frac{min}{d}*2} = 386.42\frac{l}{min} \quad (single\ wing\ flow\ rate) \tag{2.3}$$

$$N_{re} = \frac{w*u*\rho}{\mu} \qquad where \tag{2.4}$$

$$u = \frac{q}{A} = \frac{q}{2*h*w} \tag{2.5}$$

To calculate the flow rate in the lab, we set

$$N_{re,field} = N_{re,lab} \tag{2.6}$$

which equates to

$$\frac{q}{h}(lab) = \frac{q}{h}(field) \tag{2.7}$$

$$q_{lab} = \frac{q_{field}}{h_{field}} * h_{lab} = \frac{386.42*0.142}{300} = 0.174\ \frac{l}{min} \tag{2.8}$$

Table 2.4—Laboratory flow rates for different reservoir rates

Reservoir Flow Rate, bbl/d	Lab Flow Rate, l/min
7,000	0.174
15,000	0.375
30,000	0.75

Table 2.4 shows the results of the scaled flow rates for different reservoir flow rates. A range of 0.174 to 0.75 l/m was determined as the appropriate flow rate range for this set of experiments.

2.3.6 Cyclic Stress Loading

Certain cyclic stress conditions were implemented in this experiment to simulate the drawdown and shut-in cycles that an offshore well typically faces. A closure stress at shut-in of 3,000 psi was established while an effective stress during drawdown of 10,000 psi was used. Each stress was held for 1 hour while conductivity was measured and recorded. This further contributed to the understanding of the proppant pack degradation in the field.

2.4 Comparison of Laboratory Conditions

The development of fracture conductivity testing techniques has come a long way in terms of equipment and procedure. Cooke (1975) conducted some of the first tests to measure fracture conductivity. For his tests, he developed an apparatus that measured residue per volume of fracturing fluid where he introduced a correlation to calculate gas flow through the propped fracture by considering inertial and turbulence effects. In the experiment, proppant was packed in a vertical position as shown in **Fig. 2.13**. Although these experiments did a good job of measuring short-term conductivity of proppant packs, an apparatus or procedure for long term conductivity had not been put into place.

When different tests were performed to study long term conductivity it was found that pressure and temperature have a detrimental effect on conductivity which was not obvious in short term tests. In 1989, API published the standard process where they introduced thin metal plates between which they packed proppant. Stimlab replaced the metal plates with an inch and a half thick core of Ohio sandstone which allowed a filter cake to build up (Much and Penny 1987). In 2007, ISO 13503-5 was developed based on the API RP-61 procedure and was published to define a long term conductivity test.

A three inch high core sample was used for conductivity measurements in this experiment. The reason for doing this was to allow better control of leak off through the rock sample and provide a more realistic scenario to the field. Long term tests were also run up to 24 hours.

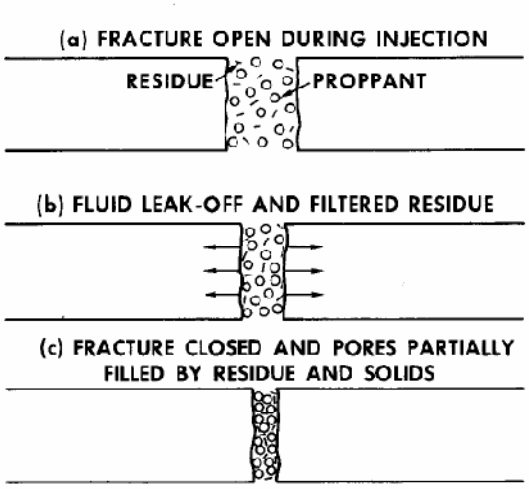

Fig. 2.13—Cooke (1975) model to simulate proppant packing

Fig. 2.14 shows the development of the core samples with different experiments. To measure conductivity, different fluids have been used based on the specific reservoir being simulated. In this experiment mineral oil with a viscosity of 10 cp was used. Flow rates were calculated between 174 and 750 ml/min compared 1-10 ml flow rates used in the past.

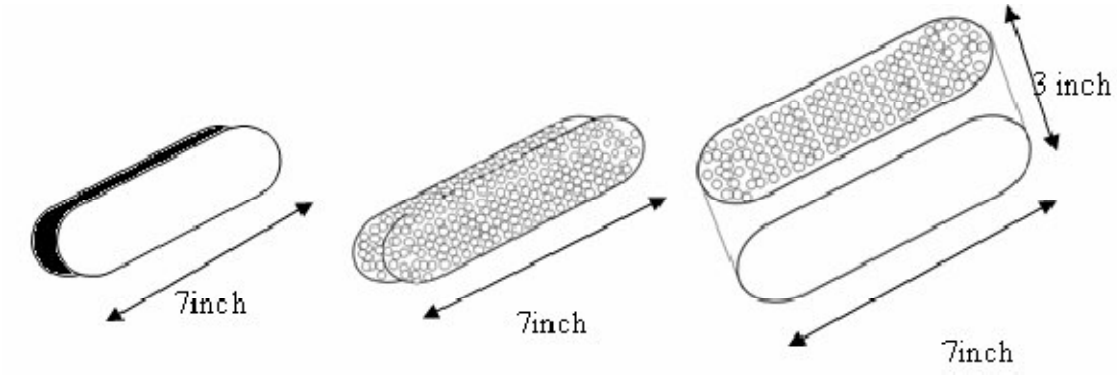

a) API RP61, 1989 b) Much and Penny, 1987 c) Pongthunya, 2007

Fig. 2.14—Core sample comparison

CHAPTER III

EXPERIMENTAL RESULTS AND DISCUSSION

All experiments were run using Berea sandstones with a high proppant concentration pack placed manually between two core samples. Each experiment used heavy brine fracture fluid which was pumped through the conductivity cell heated to 235°F. 210°F oil was then pumped through the proppant pack for each experiment and conductivity measurements were taken at various closure stresses for up to 24 hours at each stress. These experiments were run to determine the behaviors of different proppant types at high temperature and high closure stress. The conductivity values of each experiment are discussed and presented in the following section. Additional photos and data collected can be found in Appendix A.

3.1 Long Term Fracture Conductivity

High permeability hydraulic fractures are high proppant concentration fractures and are expected to have higher conductivities. Conductivity measurements taken for an hour or two do not provide an accurate estimate of fracture conductivity and therefore running these tests for over 20 hours at each stress was essential to better understand the effects of flow and proppant behavior.

In these experiments proppant concentrations were placed at 8 lb/ft^2 and 4 lb/ft^2 using uncoated and resin coated proppant. A 43.6 lb/Mgal delayed crosslinked fluid was pumped into the fracture with leak off through the cores at a temperature of 235°F to build a filter cake. Closure stress was applied to the cell and 10 cp mineral oil was pumped through the fracture to study clean-up and proppant pack behavior. It was noticed that clean-up took about 5 minutes due to the fluid being pumped, followed by conductivity values being recorded.

Fig. 3.1, 3.2, 3.3 and **3.4** show the conductivity values with respect to time at each closure stress. Conductivity was measured at each closure stress with increasing order (3,000 psi, 5,000 psi, 8,000 psi, 10,000 psi). The determined rate at which the closure stress was increased between each stress interval was 150 psi/min, however, this was not taken into account for the first several tests, but also did not seem to have a significant effect on tests that were rerun later with the determined stress increase rate.

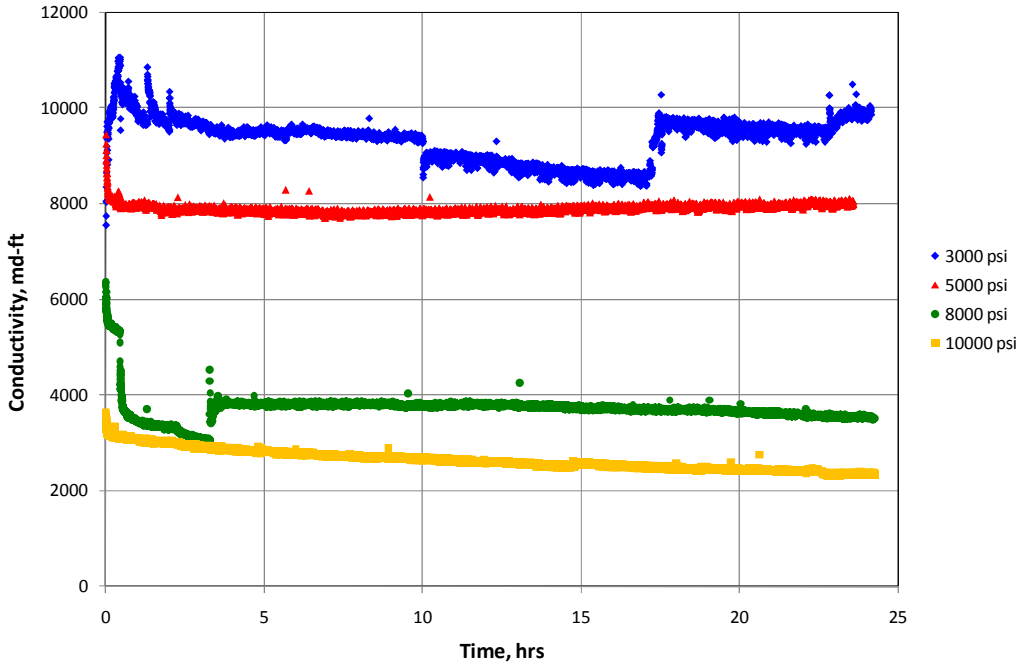

Fig. 3.1—Long term fracture conductivity study with 4 lb/ft^2 uncoated proppant

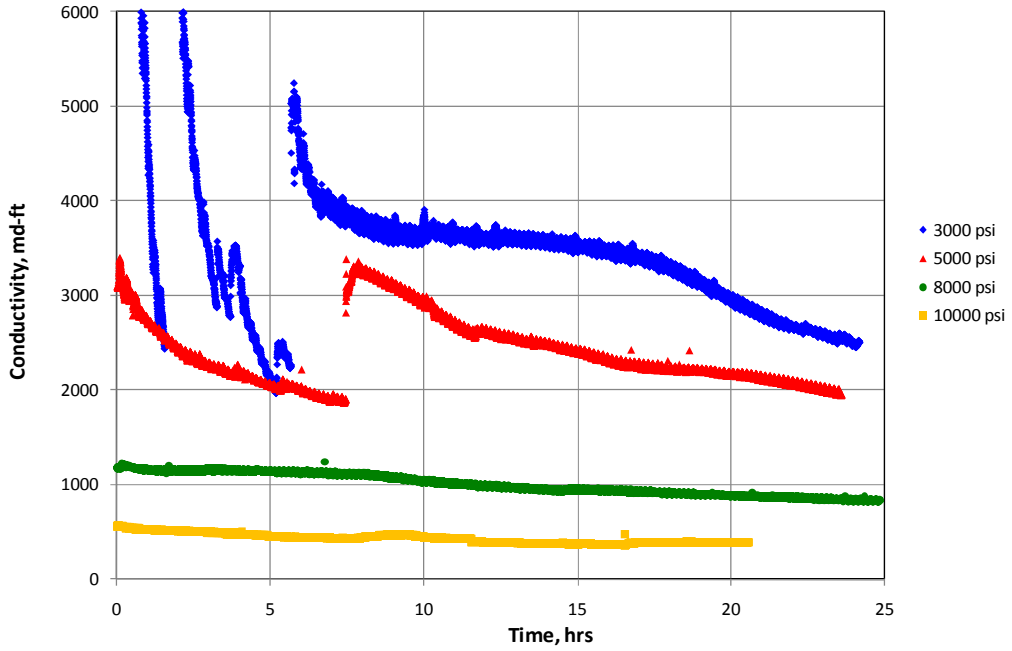

Fig. 3.2—Long term fracture conductivity study with 8 lb/ft^2 uncoated proppant

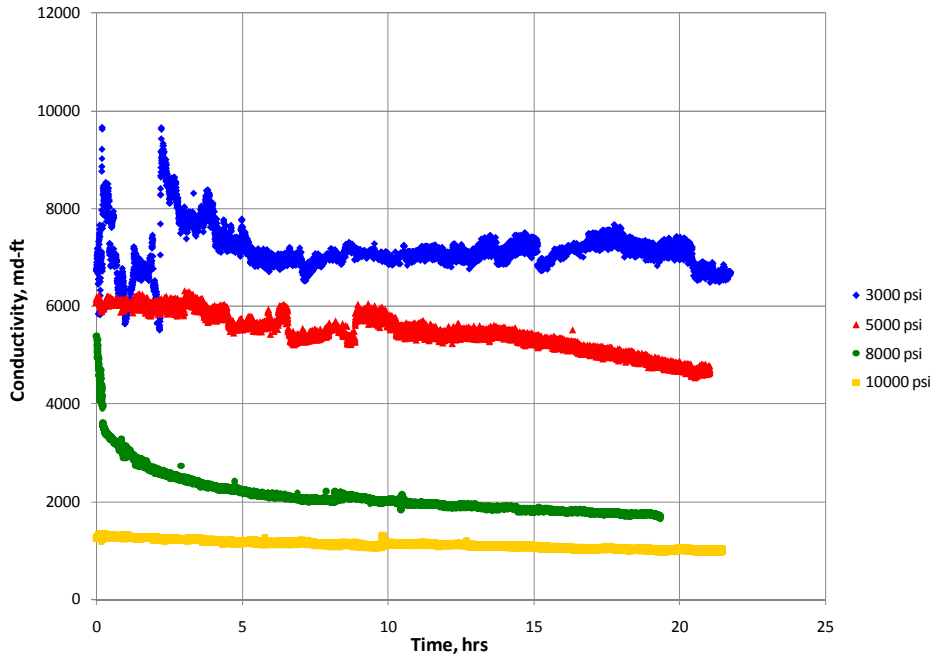

Fig. 3.3—Long term fracture conductivity study with 4 lb/ft^2 coated proppant

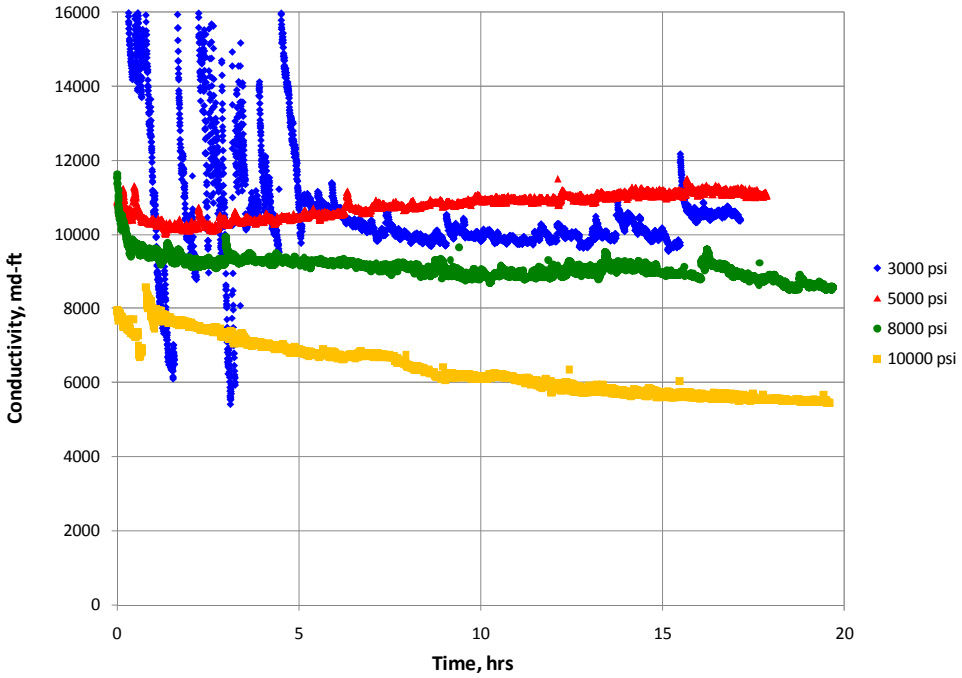

Fig. 3.4—Long term fracture conductivity study with 8 lb/ft^2 coated proppant

It was observed that increasing the closure stress for each test dramatically decreased conductivity. The 20 hour flowing time for each test also showed a further degradation in conductivity. The coated proppant tests displayed the expected increase in conductivity with increasing proppant concentration (Fig 3.3 and 3.4). The uncoated test however, did not display this. The 8 lb/ft^2 (Fig 3.2) test shows significantly reduced conductivity compared with the 4 lb/ft^2 uncoated test (Fig 3.1). The reduced conductivity will be further investigated in the following sections. **Fig. 3.5** and **3.6** below illustrates how the proppant was distributed in a typical experiment.

Fig. 3.5—Proppant distribution in the fracture with 8 lb/ft^2 of coated proppant

Fig. 3.6—Side and front view of core sample with 8 lb/ft^2 of uncoated proppant

3.2 Sieve Analyses of Proppant after Conductivity Testing

A sieve analysis of each proppant sample was taken from each long term test run in section 3.1. An analysis was done on both proppant types, uncoated and coated, prior to being subjected to the experimental conditions and then used for comparison purposes of the proppant sample taken from each experiment. The proppant samples could then be checked to quantify the amount of crushing that occurred when subjected to such high stresses and temperature. The samples were washed to remove any oil prior to the post-sieve analysis.

The results of these analyses can be found in **Fig. 3.7** and **3.8** and both show a minimal amount of proppant crushing or loss of proppant integrity. Fig. 3.7, however, the uncoated proppant analysis, shows a greater amount of crushing compared with the coated proppant analysis in Fig. 3.8. This could be the result of additional movement in the uncoated proppant pack due to the lack of static friction or adhesion provided by the resin coating of the coated proppant.

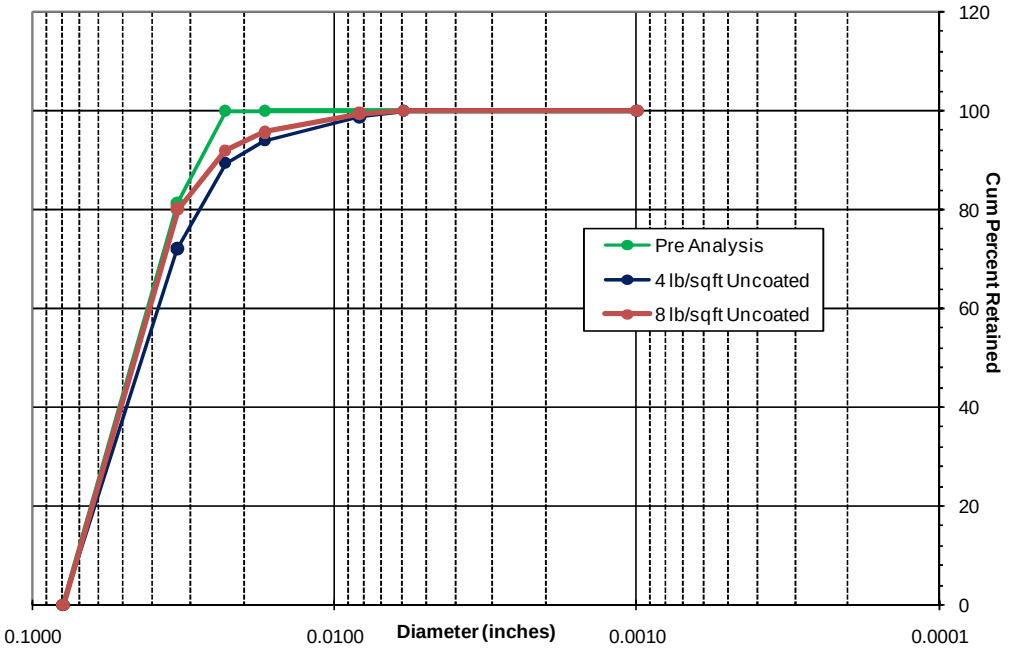

Fig. 3.7—Sieve analysis of uncoated proppants

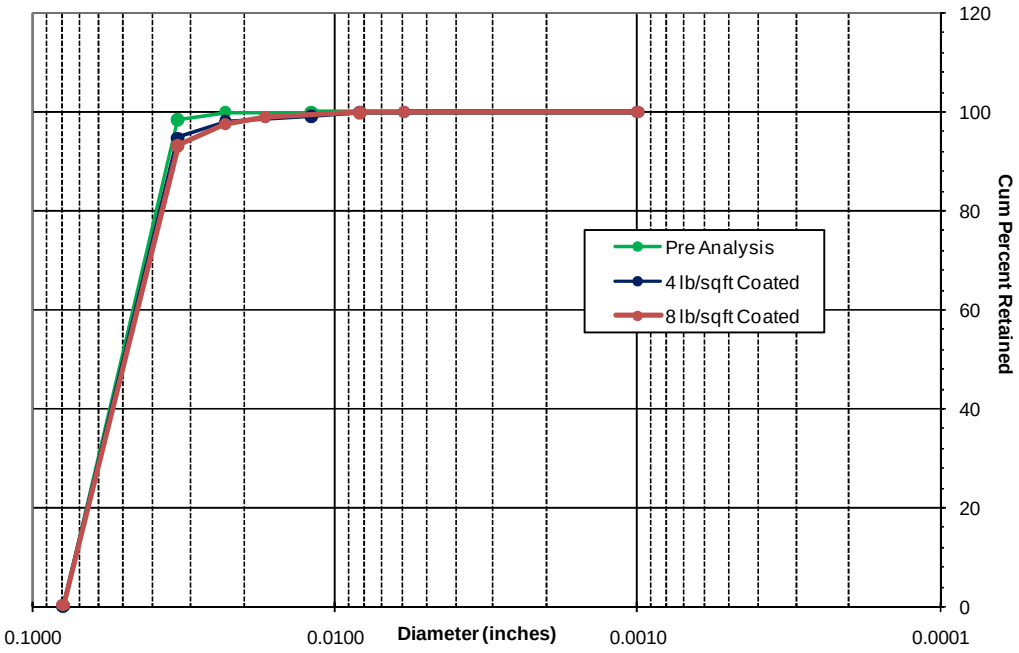

Fig. 3.8—Sieve analysis of coated proppants

3.3 Effect of Closure Stress and Proppant Concentration on Fracture Width

To further study proppant behavior, the capability to measure fracture width dynamically along with conductivity was also added. The capability was added to see if the rapid declines in conductivity with the 8 lb/ft^2 uncoated test could be related to a rapid decline in fracture width caused by proppant rearrangement or proppant rollover. A 6 lb/ft^2 uncoated test was run as a comparison to the 4 and 8 lb/ft^2 uncoated tests and fracture width was analyzed. The results of this test can be found in **Fig. 3.9, 3.10, 3.11,** and **3.12.**

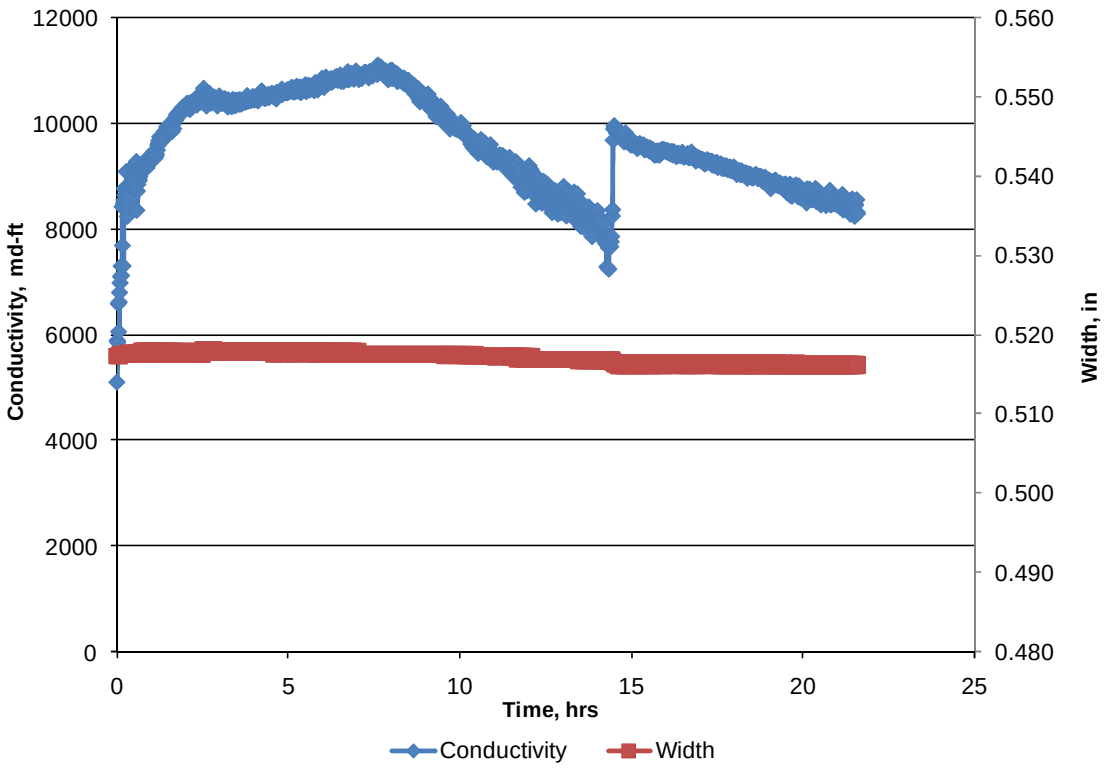

Fig. 3.9—Conductivity analysis using 6 lb/ft^2 uncoated proppant (3,000 psi)

Fig. 3.9 shows a relatively constant conductivity and width with an initial fracture width of 0.518 inches at a closure stress of 3,000 psi. Fig. 3.10 and 3.11 however exhibit a much greater decline in conductivity and fracture width when increasing to 5,000 and 8,000 psi of closure stress respectively. When the closure stress was increased to 5,000 psi (Fig. 3.10) the width decreased from 0.492 to 0.483 inches while the conductivity dropped from 8,000 to 2500 md-ft during a 22 hour period of time. Once the closure stress was increased to 8,000 psi (Fig. 3.11) there was an even greater decline in fracture width (0.440 to 0.360 inches) and conductivity (2500 to 550 md-ft) over a similar period of time. Fracture width dropped even further to 0.332 inches when the closure stress was increased to 10,000 psi (Fig. 3.12). Conductivity held at 550 md-ft, however, oil was only pumped for about 10 minutes due to equipment issues.

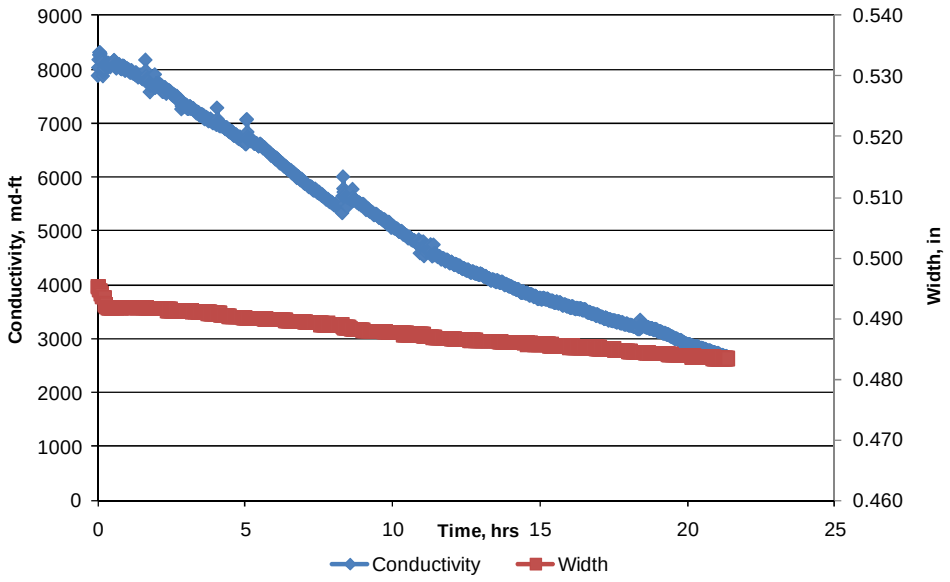

Fig. 3.10—Conductivity analysis using 6 lb/ft^2 uncoated proppant (5,000 psi)

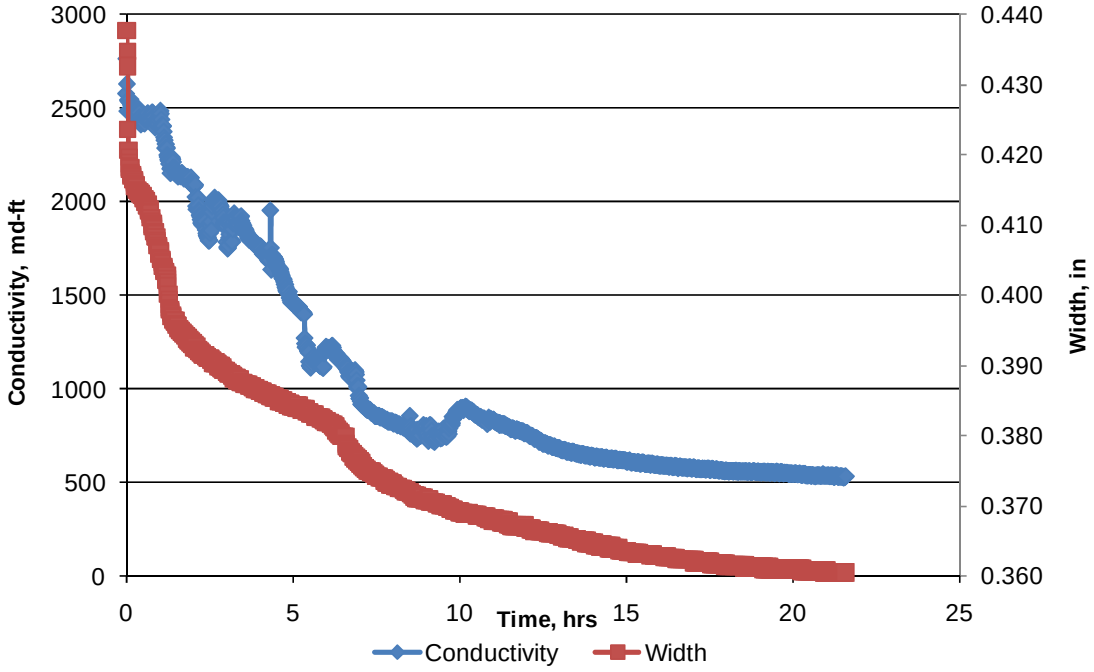

Fig. 3.11—Conductivity analysis using 6 lb/ft^2 uncoated proppant (8,000 psi)

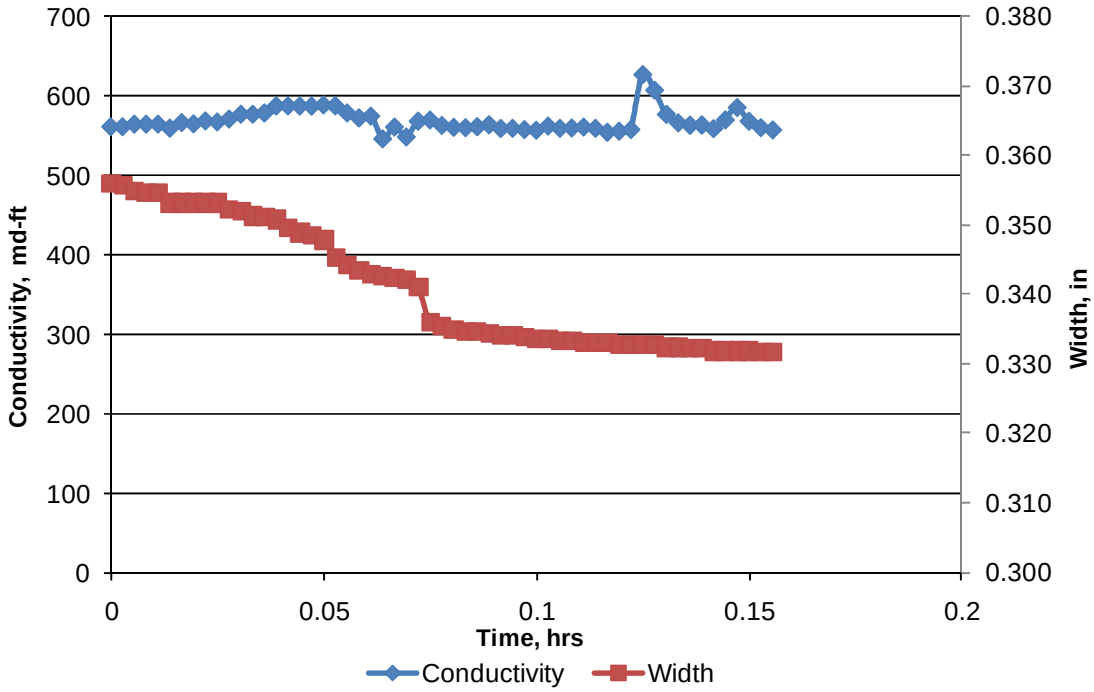

Fig. 3.12—Conductivity analysis using 6 lb/ft^2 uncoated proppant (10,000 psi)

Fig. 3.13 displays porosity of the proppant pack versus time for each closure stress for the 6 lb/ft^2 uncoated tests shown in the figures above. Observing figures 3.9-3.13 show that porosity of the proppant pack closely correlates to the conductivity and width of the proppant pack. The largest decline in conductivity occurred during the 8,000 psi interval of the test and when comparing this to Fig. 3.13 one can observe that there is a steady decline in porosity as well.

$$\phi_p = 1 - \frac{c_p}{w_p \rho_p} \tag{3.1}$$

Eq. 3.1 was the equation used to calculate porosity where (C_p) is the proppant concentration in lb/ft^2, (w_p) is the proppant pack width in ft., and (ρ_p) is the proppant density in lb/ft^3. The specific gravity of the proppant analyzed in Fig. 3.13 was 3.48.

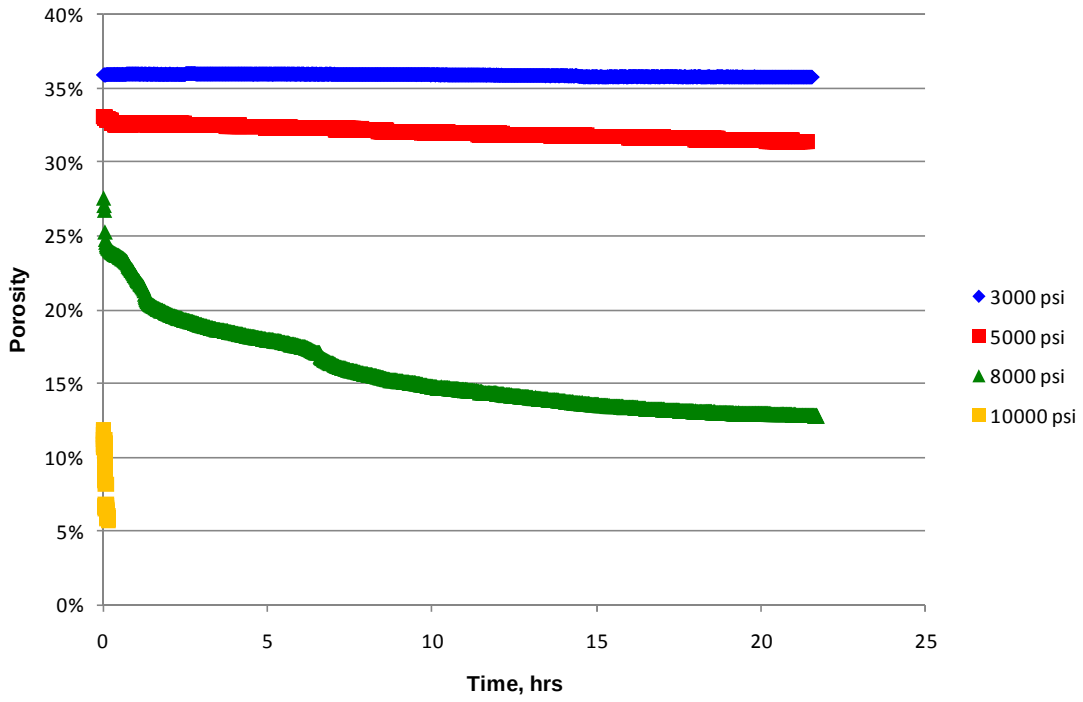

Fig. 3.13—Porosity of 6 lb/ft^2 uncoated proppant with increasing closure stress

3.4 Effect of Closure Stress and Proppant Concentration on Final Conductivity

To summarize the results of each test run it was important to analyze the final conductivity values at each closure stress for each proppant type and concentration. **Fig. 3.14** displays all of the final conductivity values for each 20 hour test run. Notice that the 8 lb/ft^2 uncoated proppant test was run an additional 2 times and again showed surprisingly low values for each test (8 lb/sqft Uncoated_2 and 8 lb/sqft Uncoated_3 shown in legend of Fig. 3.13). The 3rd test was run without the presence of fracture fluid and only had oil pumped through the proppant pack. This showed that the low values were not caused by excessive gel damage. When selecting a concentration of 6 lb/ft^2 with uncoated proppant there again appears to be very low conductivity values when comparing to the 4 lb/ft^2 uncoated test.

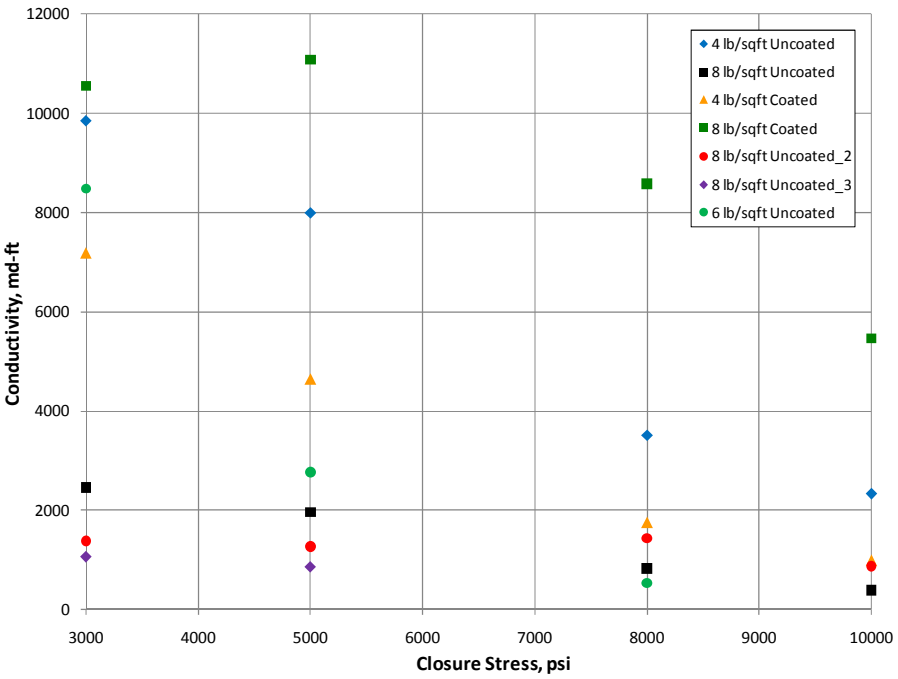

Fig. 3.14—Final conductivity values after each 20 – 24 hour test

3.5 Effect of Cyclic Loading on Conductivity

Cyclic loading of the proppant pack was also studied in certain cases after the long term tests had been completed at a closure stress of 10,000 psi. The purpose of these cyclic tests was to find out if the conductivity measured at the lower closure stresses could be regained. **Fig. 3.15** shows an example of a cyclic test (8 lb/ft^2 uncoated proppant) where after the long term test was run, the stress was cycled incrementally back down to 3,000 psi with conductivity measured at each incremental stress. Closure stress was then cycled back up to 10,000 psi and the test was stopped. Fig. 3.15 also shows that once the stress on the proppant pack was increased to 10,000 psi the conductivity measured earlier at the lower stresses could not be recovered.

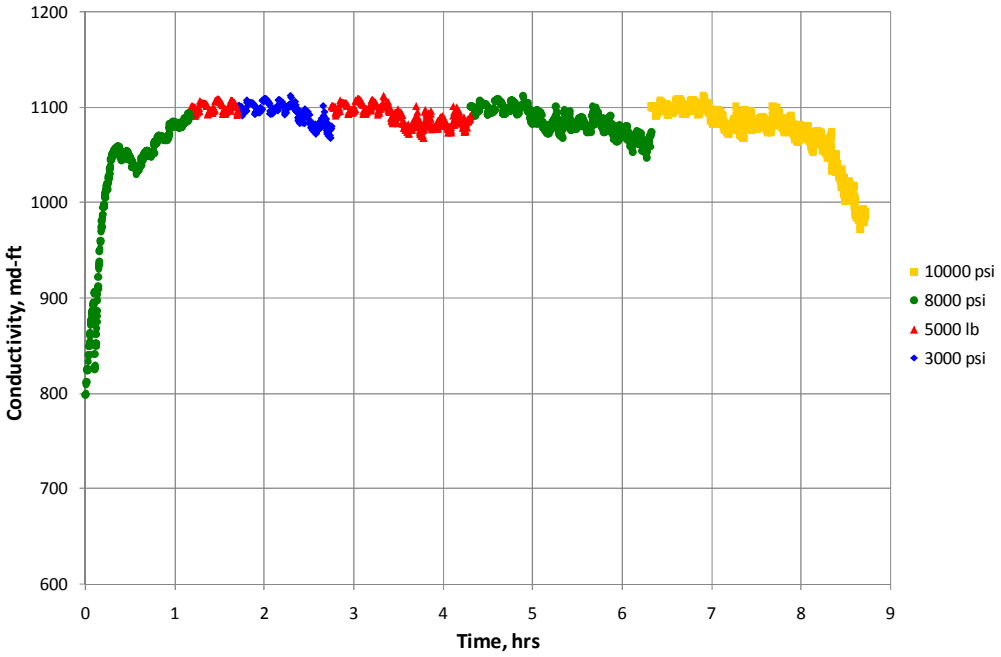

Fig. 3.15—Cyclic loading conductivity test with 8 lb/ft^2 uncoated proppant

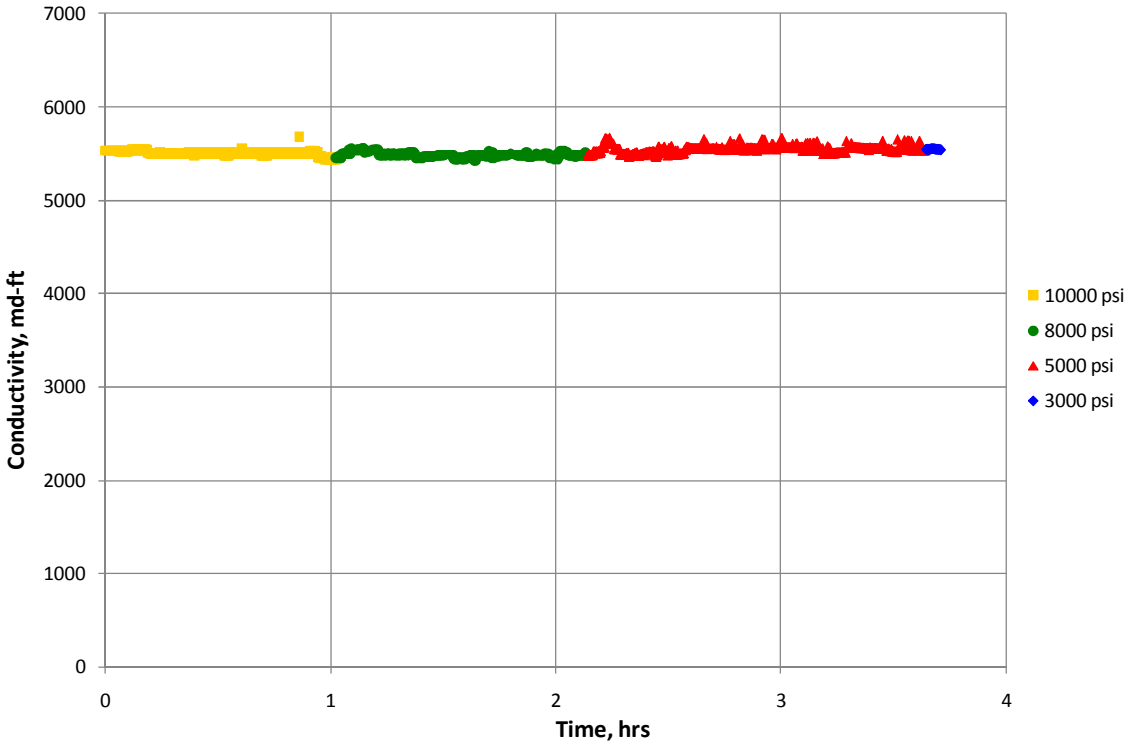

Fig. 3.16—Cyclic loading conductivity test with 8 lb/ft^2 coated proppant

Cyclic tests were also run with coated proppant at concentrations of 4 and 8 lb/ft^2 shown in **Fig. 3.16** and **3.17**. The same cyclic procedure was used, only the loading on the proppant pack was decreased from 10,000 to 3,000 psi, but not back up to 10,000 psi. The same conclusions, however, can be drawn from the results of these tests where conductvity is not regained when the closure stress is cycled back up to 3,000 psi.

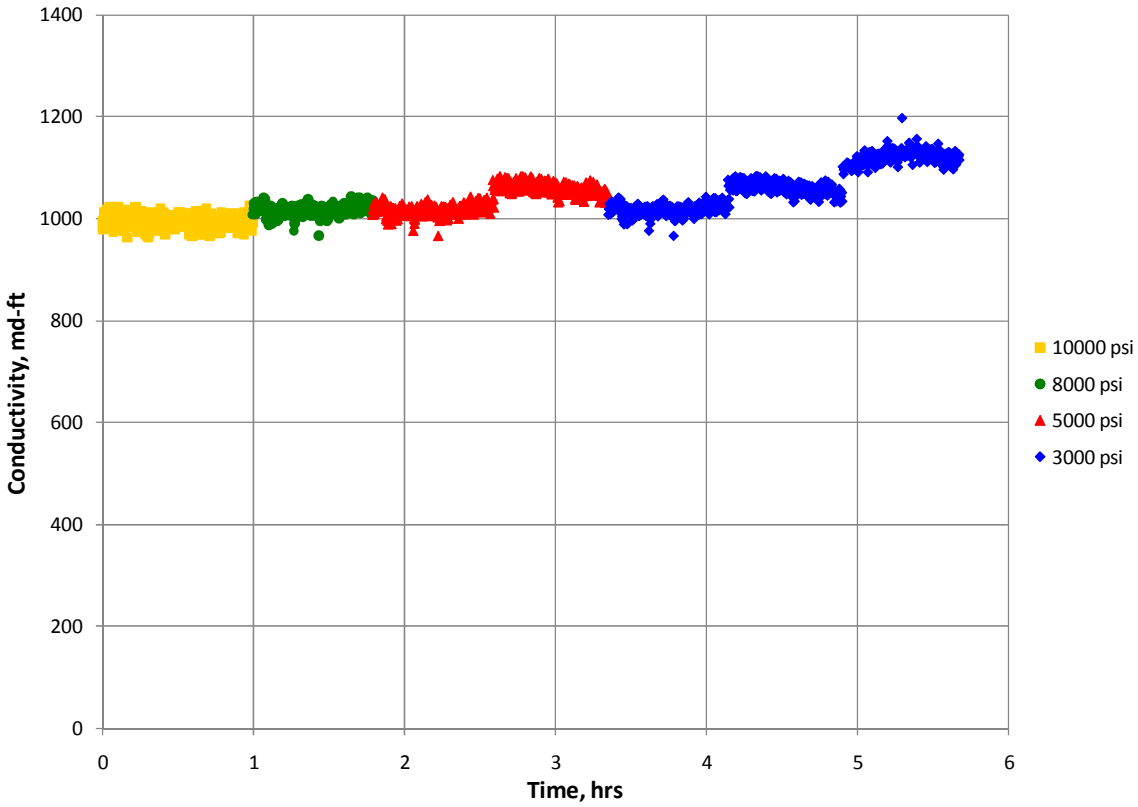

Fig. 3.17—Cyclic loading conductivity test with 4 lb/ft^2 coated proppant

3.6 Leak Off Coefficient of Berea Sandstone

Tests were also run to study the consistency of leak off when pumping the fracture fluid through the proppant pack at the beginning of the experiment. The Berea sandstone used had a permeability of around 100 md and was initially saturated with 12.3 ppg NaBr brine. The leak off collected and measured during this test was the NaBr brine that was displaced by the fracture fluid and consequent filter cake built up in the core samples. A constant pressure of 25 psi was maintained throughout the pumping process. The results from these tests can be found in **Fig. 3.18** and **3.19** and offer fairly comparable leak off coefficients of 0.0017 and 0.0013 ft/min$^{1/2}$ respectively.

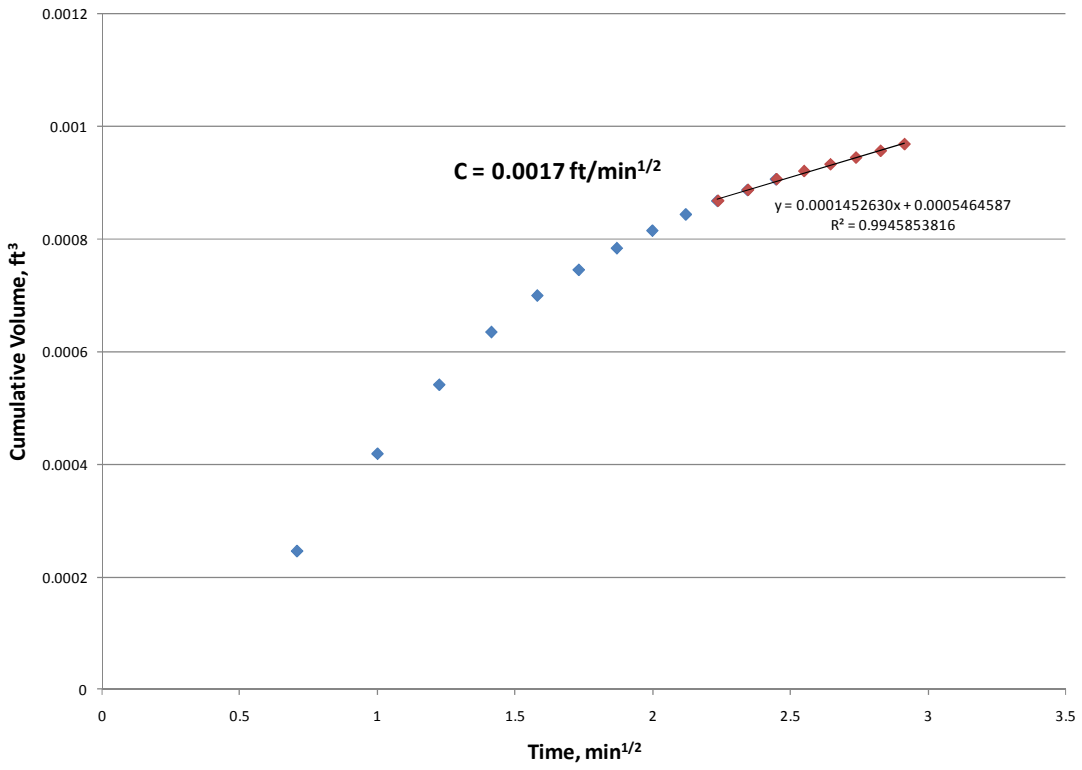

Fig. 3.18—Leak off results from 6 lb/ft^2 uncoated test

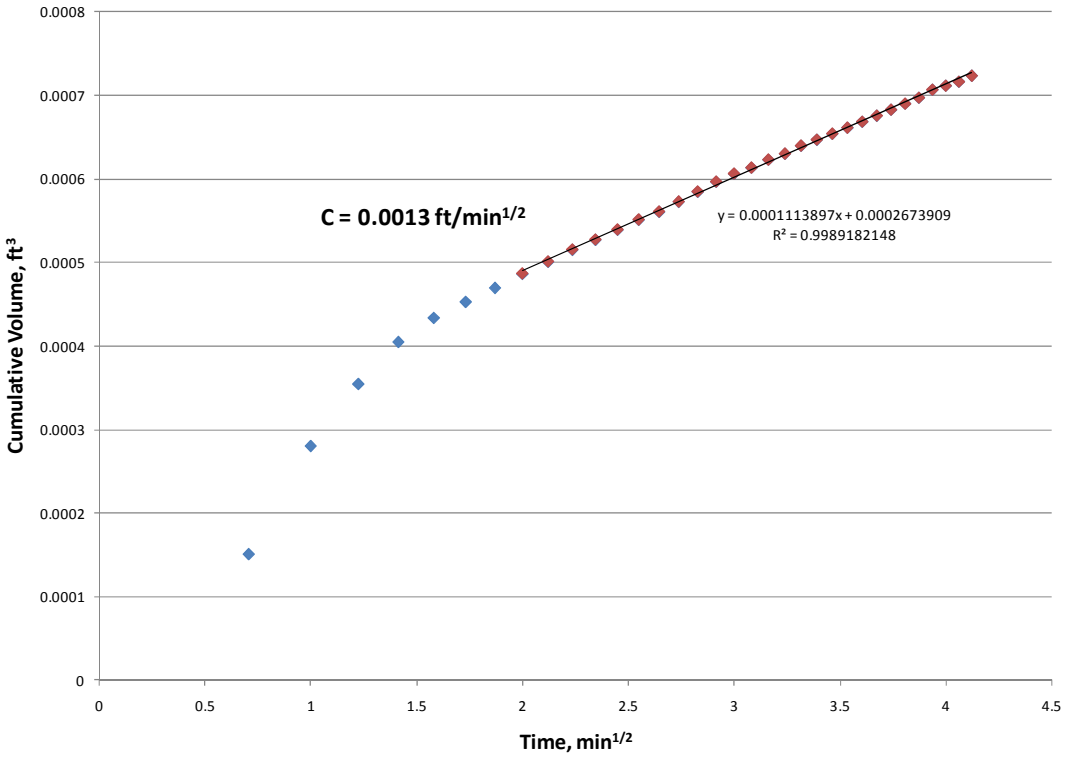

Fig. 3.19—Leak off results from 8 lb/ft^2 uncoated test

3.7 Comparison of Coated and Uncoated Proppant Performance

One of the objectives of this study was to identify some of the performance differences between coated and uncoated proppant unrelated to proppant flow back performance. The reason coated proppant was developed is to limit proppant flow back into the wellbore and therefore help sustain a level of conductivity and limit near wellbore pressure drop. Comparing the 4 lb/ft^2 tests in **Fig. 3.20**, the conductivity of the uncoated proppant is considerably higher than that of the coated proppant conductivity. When comparing the 8 lb/ft^2 tests however, the results are reversed with the uncoated proppant having an extremely low conductivity compared with the coated proppant.

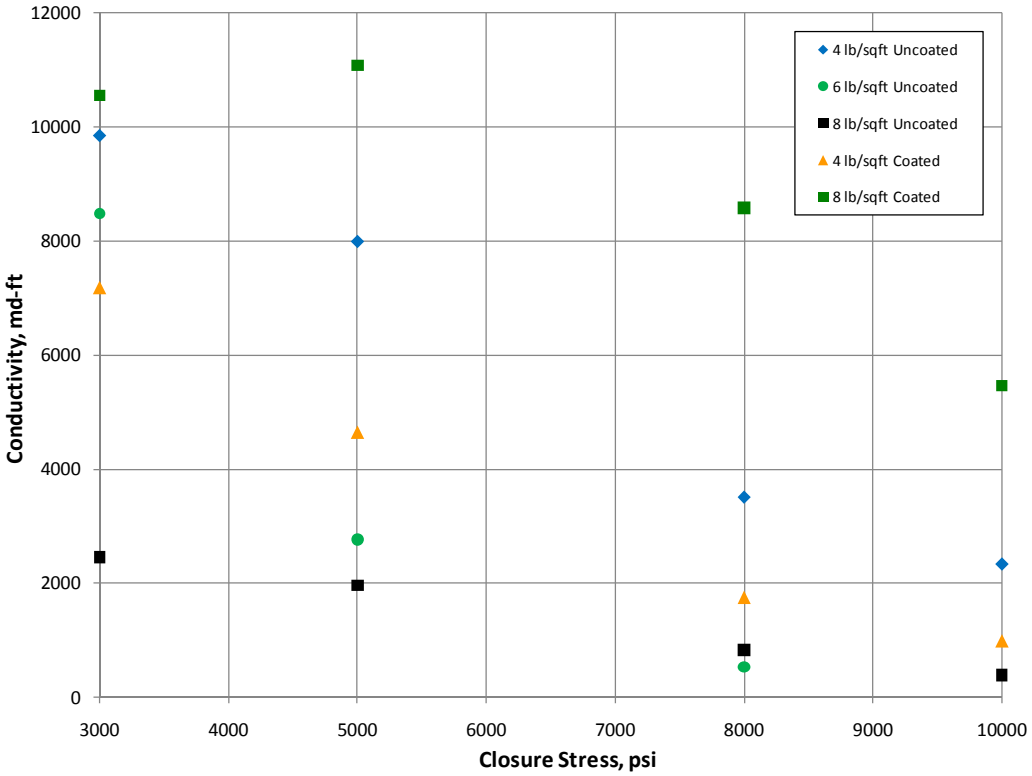

Fig. 3.20—A comparison of uncoated and coated proppant tests

The low conductivity values for the 8 lb/ft^2 uncoated tests are the result of what is believed to be proppant rearrangement and compaction due to the high fracture width. Due to the fact that there is such great distance between the cores (> 0.6 inches) in the conductivity cell, there is less static friction in the center of the proppant pack and the proppant is able to move more freely than it would be able to in a narrower fracture. The coated proppant seems to resolve the rearrangement due to the adhesion of the proppant from the resin, creating a consolidated proppant pack. The results of the 8 lb/ft^2 uncoated and coated can be compared in Fig. 3.20.

To better understand the behavior of the 16/30 uncoated proppant used in this study an analysis was performed to compare the number of layers of proppant and the respective proppant concentration shown in **Fig. 3.21**. To calculate the number of layers a rhombic packing order was assumed with a porosity of 0.27 and a nominal proppant diameter of 0.03 inches was also measured during the sieve analyses.

$$\#Layers = \sqrt{3/2}\,\frac{w_p}{\overline{d_p}} \tag{3.2}$$

Eq. 3.2 was used to calculate the number of layers using Eq. 3.1 rearranged to calculate the width for each proppant concentration.

Comparing Fig 3.20 to 3.21 will draw several conclusions. Fig. 3.21 shows that a 4 lb/ft^2 16/30 uncoated proppant pack will have about 12 layers, whereas a 6 lb/ft^2 uncoated proppant pack will have about 18 layers. Increasing from 12 to 18 layers of proppant is when the proppant rearrangement begins with the experimental conditions set for this study. The 8 lb/ft^2 proppant pack with 25 layers will have an even greater impact on proppant rearrangement and conductivity degradation.

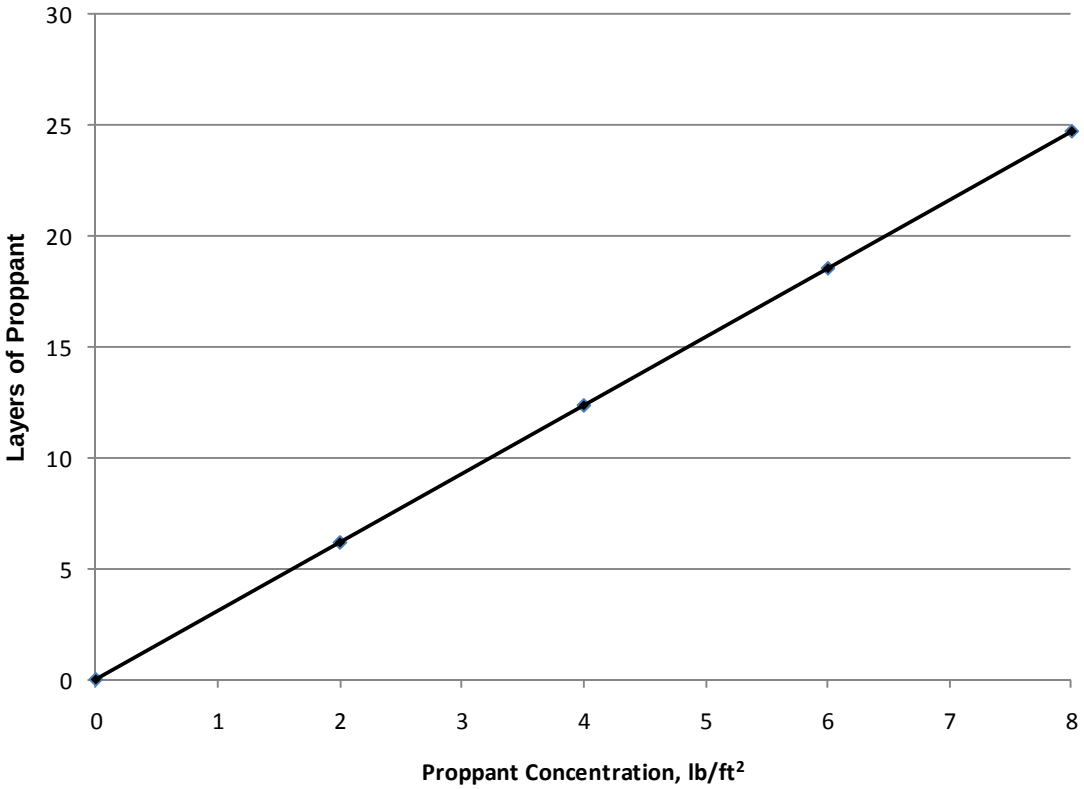

Fig. 3.21—Analysis of proppant layers versus proppant concentration

CHAPTER IV

CONCLUSIONS AND RECOMMENDATIONS

4.1 Conclusions

Long term conductivity tests were conducted with both coated and uncoated proppants for up to 24 hours at each closure stress interval, and in addition some cyclic testing was performed. The capability to measure fracture width dynamically with conductivity was added to better observe proppant behavior at high temperature and closure stress. The following conclusions are made based on the observations of the study:

1. An increase in closure stress will have a significant impact on fracture conductivity due to compaction of the proppant pack.
2. There is a significant link between the compaction of the proppant pack and the decrease in conductivity which was verified by dynamically measuring the fracture width with the conductivity of the fracture. This was also verified by calculating the porosity.
3. When increasing the closure stress on the proppant pack to 10,000 psi there is not a significant amount of crushing, however, the uncoated proppant does degrade slightly more than the coated proppant as verified by the sieve analyses. This is most likely due to the added static friction or adhesion of the coated proppant which discourages the rearrangement and rolling over of the proppant.

4. Cycling the closure stress after reaching the maximum closure stress (10,000 psi) will not regain the previous conductivity values at the lower closure stresses. This is due to irreversible damage and compaction of the proppant pack.
5. A reasonable and repeatable leak off coefficient was measured using the set up apparatus with cross linked gel and a fairly low pressure (25 psi). Different cores with different fracture fluids could be used to compare various leak off environments.
6. When increasing the concentration of the uncoated proppant there is a clear and repeatable loss in conductivity under experimental conditions. Higher concentrations of uncoated proppant will therefore have a lower conductivity than that of lower concentrations of uncoated proppant.
7. When analyzing the number of layers of uncoated proppant at different concentrations and comparing them to the conductivity tests, there in a loss in conductivity when increasing from 12 layers of proppant to 18 layers of proppant. The layers correspond to 4 lb/ft^2 and 6 lb/ft^2 respectively.
8. There is a definite difference in performance when comparing uncoated and coated proppants at lower concentrations. Uncoated proppant provides a higher conductivity than coated proppant. This is likely due to the resin from the coated proppant causing a reduction in porosity due to the consolidation of the proppant pack.

4.2 Recommendations

The experiments conducted produced many conclusions; however, additional testing under different conditions would add further valuable conclusions. Berea sandstone was used during these experiments to attempt to replicate the actual reservoir when it would be more ideal to use actual core from the field. There is also some equipment that could be added to make the procedure of the experiment more consistent.

Cyclic testing was performed for some of the experiments conducted; however, there could be a more extensive investigation of the effects of cyclic stress on the proppant pack. In the field of study a closure stress at shut-in of 3,000 psi was established while there is an effective stress during drawdown of 10,000 psi. Each stress could be held for 5 hours while conductivity and fracture width are measured and recorded. The experiment would cycle the stresses to simulate the shut-in and consequent drawdown 5 times. This would further contribute to the understanding of the proppant pack degradation in the field.

Different proppants could be used to further expand the study. Higher strength proppants such as bauxite could be used to understand if there would be a lesser degradation to the proppant pack. In this study only coated and uncoated high strength ceramic proppant were used. The proppant size could also be varied to study its effects on proppant pack conductivity.

A newer load frame that would be programmable to adjust the closure stress on the proppant pack and simultaneously record pressure drop, fracture width, temperature, and flow rate would reduce the operator's required time spent in the lab. An electronic

feedback controller to regulate the flow rate of the oil along with a coriolis flow meter would also reduce the potential for inconsistencies. The combination of these devices, along with proper set up would automate a large portion of the experiment. One experiment requires about 100 hours of pumping.

REFERENCES

Aggour, T. 2001. Optimization Strategies for Hydraulic Fractures in High Permeability Reservoirs. Paper SPE 68131 presented at the SPE Middle East Oil Show, Bahrain, 17-20 March. DOI: 10.2118/68131-MS.

Barmatov, E., Abbott, J., Golovin, A., Kalinin, S., Straz, E., Usova, Z. 2008. Setting the Standard for Resin Coated Proppant Testing. Paper SPE 115547 presented at the SPE Russian Oil and Gas Technical Conference and Exhibition, Moscow, Russia, 28-30 October. DOI: 10.2118/115547-MS.

Cooke Jr., C.E. 1975. Effect of Fracturing Fluids on Fracture Conductivity. *J. Pet Tech* **27** (10): 1273-1282. SPE-5114-PA. DOI: 10.2118/5114-PA.

Freeman, E.R., Anschutz, D.A., Rickards, A.R., Callanan, M.J. 2009. Modified API/ISO Crush Tests with a Liquid-Saturated Proppant under Pressure Incorporating Temperature, Time, and Cyclic Loading: What Does It Tell Us? Paper SPE 118929 presented at the SPE Hydraulic Fracturing Technology Conference, The Woodlands, Texas, 19-21 January. DOI: 10.2118/118929.

Hunt, J.L., Chen, C., Soliman, M.Y. 1994. Performance of Hydraulic Fractures in High Permeability Formations. Paper SPE 28530 presented at the SPE Annual Technical Conference and Exhibition, New Orleans, Louisiana, 25-28 September. DOI: 10.2118/28530-MS.

Kaufman, P.B., Anderson, R.W., Parker, M.A., Brannon, H.D., Neves, A.R., Abney, K.L., Joyce, S.A., Ziegler, M.J., Kerr de Paiva Cortes, G.W., Penny, G.S. 2007. Introducing New API/ISO Procedures for Proppant Testing. Paper SPE 110697 presented at the SPE Annual Technical Conference and Exhibition, Anaheim, California, 11-14 November. DOI: 10.2118/110697-MS.

McDaniel, B.W. 1986. Conductivity Testing of Proppants at High Temperature and Stress. Paper SPE 15067 presented at the SPE California Regional Meeting, Oakland, California, 2-4 April. DOI: 10.2118/15067-MS.

Much, M.G., Penny, G.S. 1987. Long-Term Performance of Proppants under Simulated Reservoir Conditions. Paper SPE 16415 presented at the SPE Low Permeability Reservoirs Symposium. Denver, Colorado, 18-19 May. DOI: 10.2118/16415-MS.

Palisch, T.T., Duenckel, R.J., Bazan, L.W., Heidt, J.H., Turk, G.A. 2007. Determining Realistic Fracture Conductivity and Understanding Its Impact on Well Performance - Theory and Field Examples. Paper SPE 106301 presented at the SPE Hydraulic Fracturing Technology Conference, College Station, Texas, 29-31 January. DOI: 10.2118/106301-MS.

Roodhart, L.P., Fokker, P.A., Davies, D.R., Shlyapobersky, J., Wong, G.K. 1994. Frac-and-Pack Stimulation: Application, Design, and Field Experience. J. Pet Tech **46** (3): 230-238. SPE-26564-PA. DOI: 10.2118/26564-PA.

RP 61, Recommended Practices for Evaluating Short Term Proppant Pack Conductivity, 1989. Washington DC: API.

Stephens, W.T., Schubarth, S.K., Dickson, K.R., Snyder, E.M., Doles, K., Herndon, D.C. 2007. Behavior of Proppants under Cyclic Stress. Paper SPE 106365 presented at the SPE Hydraulic Fracturing Technology Conference, College Station, Texas, 29-31 January. DOI: 10.2118/106365-MS.

APPENDIX

A.1 – Experimental Setup

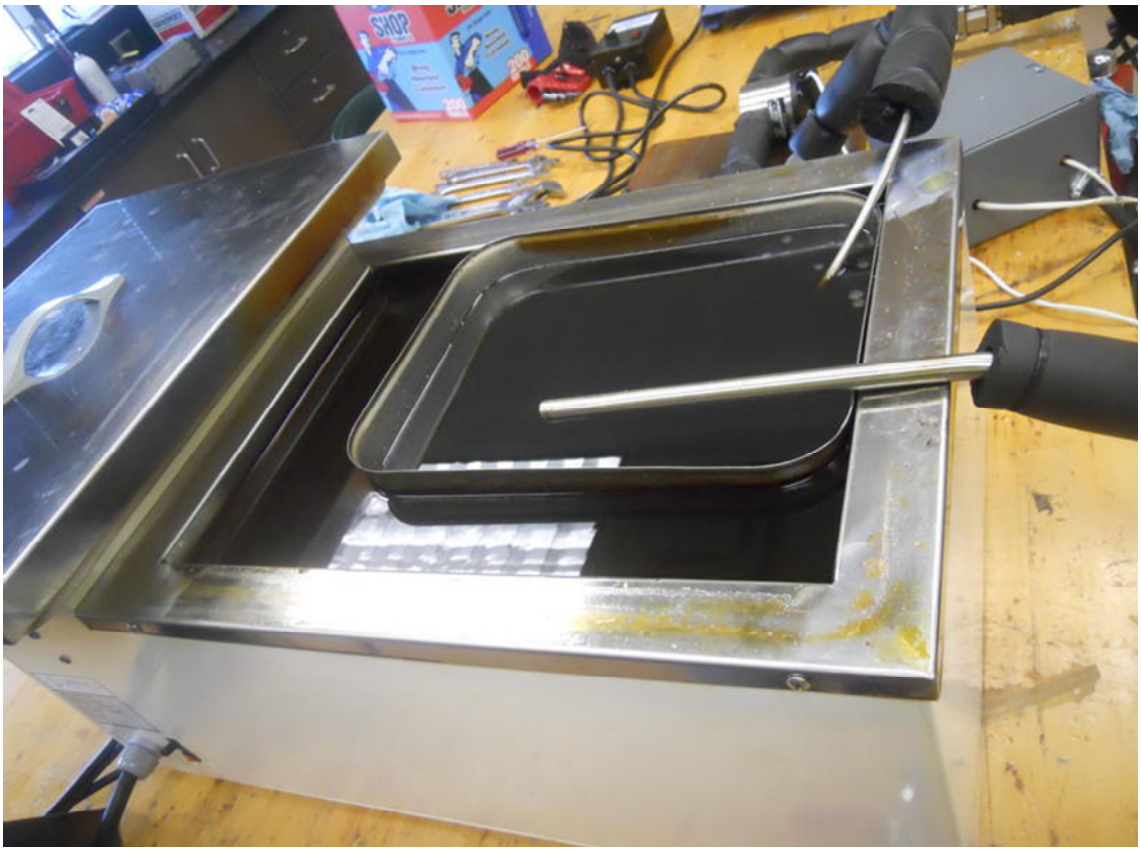

Fig. A.1.1—Mineral oil heating oil bath assembly

A.2 – Experimental observation from 8 lb/ft^2 Coated Test

Fig. A.2.1—Consolidated coated proppant collected after test

A.3 – Experimental data for 8 lb/ft^2 Uncoated Test 2

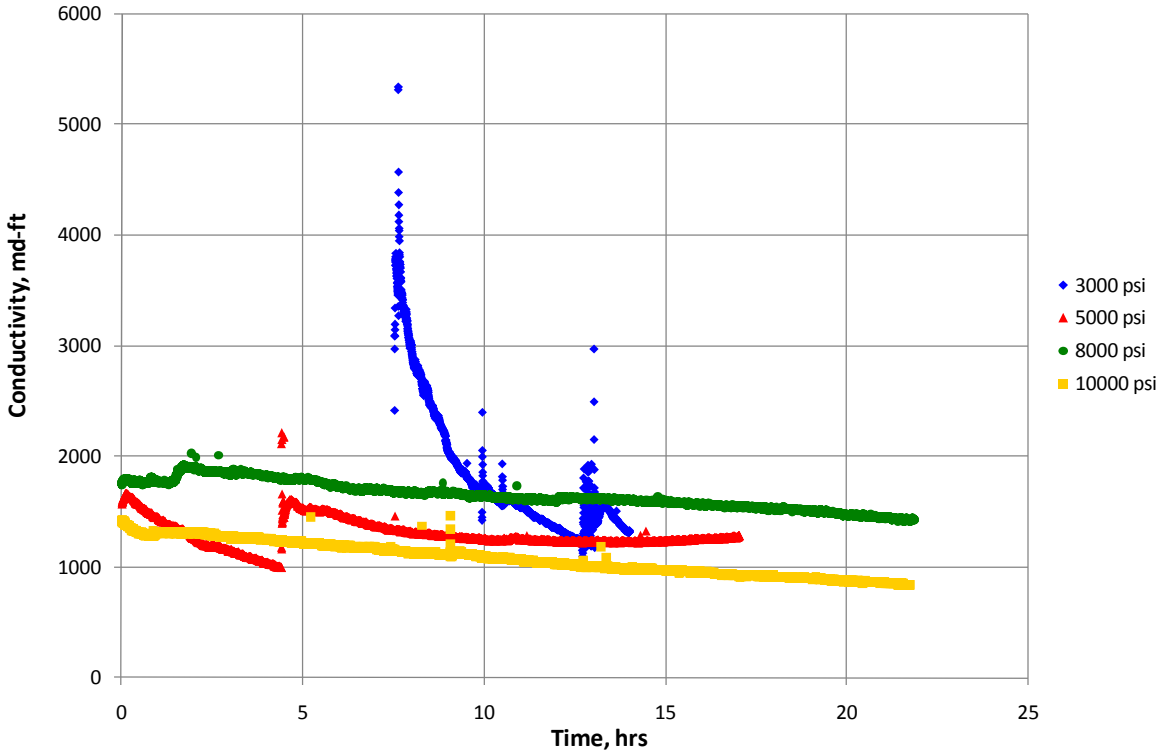

Fig. A.3.1—Results of 8 lb/ft^2 uncoated test 2

A.4 – Experimental data for 8 lb/ft^2 Uncoated Test 3

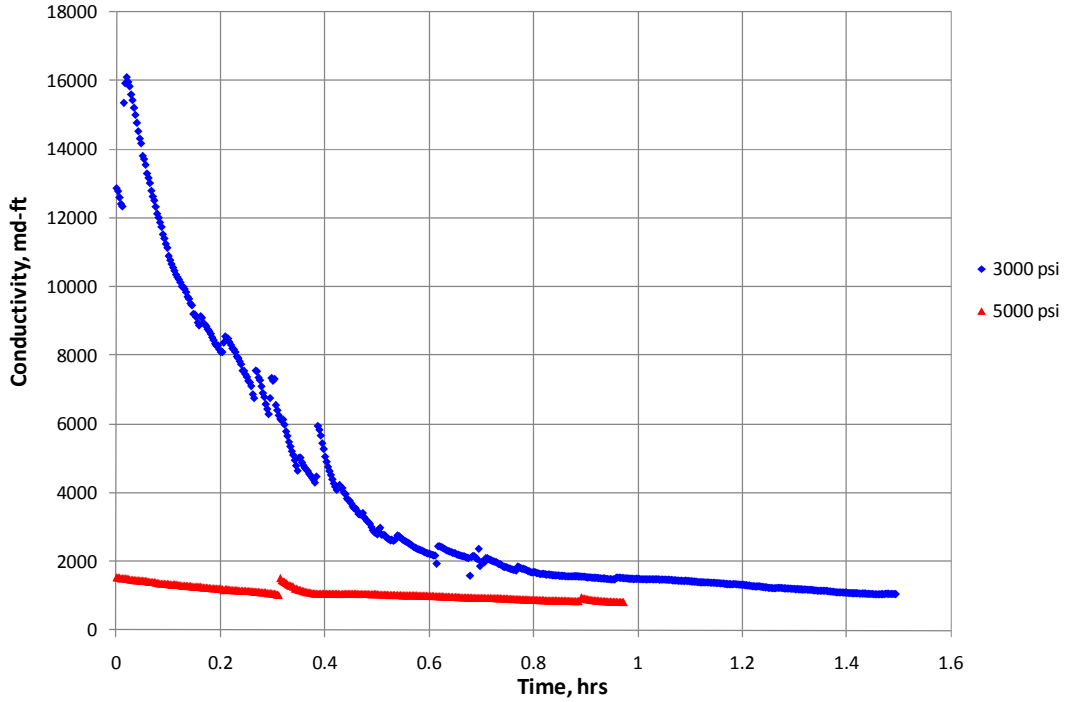

Fig. A.4.1—Results of 8 lb/ft^2 uncoated test 3

A.5 – Experimental observation from 6 lb/ft^2 uncoated Test

Fig. A.5.1—Bottom core surface where oil was flowing

VITA

Name: Matthew Charles Rivers

Address: Texas A&M University
Petroleum Engineering Dept.
3116 TAMU 501 Richardson Bldg.
College Station, TX 77843

Email Address: riversma@ameritech.net

Education: B.S., Mechanical Engineering,
Michigan State University, 2006

M.S., Petroleum Engineering,
Texas A&M University, 2010

This thesis was typed by the author